Modelling the behaviour of conventional and heavy Rydberg atoms in a Stark field

Jeffrey Philippson

Supervisor: Dr Ralph Shiell
Department of Physics & Astronomy
University of Sussex

Dissertation submitted for the Degree of Master of Physics from the University of Sussex

· 2004 ·

Abstract

The boundary between the classical and quantum domains in conventional and heavy Rydberg atoms is investigated through modelling of their response to the application of a Stark field. The applicability of a reduced mass, single particle model of the heavy Rydberg atom is constructed and its behaviour is compared with the conventional Rydberg atom.

Contents

List of Figures

Acknowledgments

I would like to thank the many people whose help and support has made this project possible.

First and foremost I would like to acknowledge the patience of my project tutor Dr Ralph Shiell over the past 6 months.

Particular thanks are also due to:

Prof. A. V. Sobolev

Prof Gabriel Barton

Daniel Neame

Chapter 1

Introduction

1.1 The conventional Rydberg atom

The general definition of a conventional Rydberg atom found in most atomic physics books refers to atoms of high principle quantum number n. While this does give a general idea of what a Rydberg atom is, it does not explain their significance.

Rydberg atoms are atoms with exaggerated properties and as such are easily detected. Their similarity to hydrogen makes them extremely useful for investigating the properties of other atoms by analogy with the well understood hydrogen system. In spite of its shortcomings, the Bohr model of the atom does explain the exaggerated properties that first identified Rydberg atoms as a topic of interest. Classically an electron in a circular orbit of radius r, about a nucleus of charge Ze, obeys Newtons 2nd law

$$\frac{mv^2}{r} = \frac{kZe^2}{r^2}. \tag{1.1}$$

In S.I. units $k = \frac{1}{4\pi\varepsilon_0}$. S.I. units are used throughout this report and this particular substitution will be used regularly.

The orbital angular momentum is quantised in units of $\hbar$

$$mvr = n\hbar. \tag{1.2}$$

Combining these two equations leads to equation 1.3 which is Bohr's expression for the radius of the orbit in terms of the principle quantum number n, from which the Bohr radius a_0 is derived $\{a_0 = r(n = 1, Z = 1)\}$

$$r = \frac{n^2\hbar^2}{kZe^2m}. \tag{1.3}$$

Combining the kinetic and potential energies and then substituting in the expression for the radius, gives

$$W = \frac{1}{2}mv^2 - \frac{kZe^2}{r} = -\frac{Ry}{n^2} \tag{1.4}$$

where

$$Ry = \frac{k^2Z^2e^4m}{2\hbar^2}.$$

It is now apparent why Rydberg atoms have such peculiar properties; the radius of the orbit increases as n^2 (the $n = 137$ state of hydrogen has an atomic radius $\sim 1\mu$m) and the geometric cross-section as n^4, meaning that atoms with high n are extremely large, with loosely bound valence electrons, easily perturbed or ionized by collisions and external fields; these properties make Rydberg atoms ideal for experimental atomic physics as they are comparatively easy to detect.

Atoms in fairly low energy states ($n < 15$) can be detected through fluorescence, as their short lifetimes give reasonable photon counts, prevent them passing out of view before decaying and are not significantly affected by black-body radiation

$$\tau \propto n^\alpha \tag{1.5}$$

where $\alpha \approx 3$ but varies slightly with l [1].

The detection of more highly excited atoms is generally through ionisation, allowing detection of either the electron or the positive ion, as the amplitude of a fluorescence signal is low at high n and the lifetimes are relatively long. The

lifetime for a state with $n = 100$ averaged over the component angular momentum states has been measured as 17 seconds. [2]

1.1.1 The classical view of Rydberg atoms

An atom in a state of high n has a valence electron in a large orbit far from the ion core; in such an orbit, the outermost electron feels an almost hydrogenic, $1/r$ coulomb potential from a compact ion core consisting of nucleus with Z protons and the lower electron shells filled with $Z - 1$ electrons. I will be using a new definition of the Rydberg atom, based on the similarity of the effective potential 'seen' by the outer electron to the hydrogen potential.

There are three noteworthy exceptions to this new definition, in which a Rydberg atom displays a significantly non-hydrogenic potential. In a double Rydberg state a second electron is excited into a state with an orbital radius almost as large as the first (i.e. two highly excited valence electrons); in such a state their influence on each other gives rise to a significant deviation from the simple geometry of the $1/r$ potential. The second exception occurs when the outer electron passes close enough to the ion core to polarize the inner electron states, giving rise to a $1/r^3$ dipole term in the potential:

$$V \propto \frac{A}{r} + \frac{B}{r^3} \tag{1.6}$$

where A & B are constants.
This effect is most pronounced when inner electrons on orbits of different angular momentum, have similar energy. The third exception occurs when the outer valence electron penetrates the inner electron shells shielding the nucleus, this effect is investigated in chapter 3.

1.1.2 The quantum mechanical picture

Quantum mechanically a state of high n refers to an atom in which the valence electron(s) have been excited into a formerly unpopulated electron orbital with higher energy and lower binding energy

$$E_B \propto \frac{1}{n^2}$$

Studying atoms in a state such as this allows comparisons to be drawn with the well understood hydrogen atom.

The long lifetimes of Rydberg states with high orbital angular momentum can be explained in terms of the overlapping of wavefunctions. The wavefunction of an electron in an high l state (i.e. high angular momentum) has very little overlap with the wavefunctions of the inner electrons and remains relatively unperturbed.

The three exceptions to our new definition described above, have an alternative, quantum mechanical explanation. If a second electron is excited into a high state n_i, energetically close to the state of the outer electron n_o, then its wavefunction become almost as large as the first (a double Rydberg state). This occurs as n_i approaches n_o and leads to a condition where the size of the two electron's orbits are related; a condition Gallagher refers to as *radial correlation* [1]. As hydrogen has only a single electron and therefore cannot become radially correlated, double Rydberg states do not conform to our new definition.

The second exception; polarization of the ion core described in section 1.1.1, produces an anisotropic dipole potential that causes an *angular correlation* between the motions of the two outermost electrons. This can be thought of as a tidal locking effect due to a non-spherically symmetric potential.

The wavefunction of the outer electron in states with low orbital angular momentum l is periodically localised within the shells of inner electrons and interact directly with the full charge of the nucleus.

1.1.3 What makes Rydberg atoms worth studying?

Experimental atomic physics

Although the interesting nature of Rydberg atoms has been understood since the development of the Bohr model in 1913; for a long time there was no efficient method for producing large, single-state, mono-energetic populations. There were a number of interesting experiments done in the 1950s and 1960s using electron

impact excitation:

$$e^- + A \longrightarrow A^* + e^-$$

and charge exchange excitation:

$$A^+ + B \longrightarrow A^* + B^+$$

however these techniques both produce populations with a very broad spread of energies.

The arrival of tunable dye lasers in the 1970s allowed a much greater level of control over populations of excited atoms. In optical excitation the incident photon is absorbed by the atom, thus absolutely specifying the energy of the state produced; in collisional excitation there is no control over what fraction of incident kinetic energy is transferred to the bound electron. The unprecedented control over Rydbergs states allowed by optical excitation has played a significant role in bringing the level of understanding in atomic physics to where we are today.

Investigating diamagnetic effects

The large sizes and low binding energies of Rydberg atoms lead to a high magnetic susceptability χ. As diamagnetic effects scale with the area of the orbit and the area is proportional to the radius squared ($\Rightarrow A \propto n^4$), effects impossible to detect in ground state atoms become obvious in Rydberg atoms, which demonstrate very large diamagnetic shifts.

Rydberg atoms in plasmas

Rydberg atoms form commonly in plasmas due to the recombination of electrons and positive ions; low energy recombination results in fairly stable Rydberg atoms, while dielectric recombination of electrons and positive ions with high kinetic energy often form autoionising Rydberg states (see section 4.1.2). Rydberg atoms' large sizes and susceptability to pertubation and ionisation by electric and magnetic fields, are an important factor determining the properties of plasmas.

Rydberg atoms in astrophysics

In the time between the early absorption spectroscopy experiments and the arrival of tunable lasers, interest in Rydberg atoms was kept alive by the realisation that they are common in interstellar space, and as such are an important radiation source for astronomers.

The density within interstellar gas clouds is typically many orders of magnitude lower than the best labratory vacuums attainable on Earth, allowing Rydberg atoms to persist for long periods of time without being ionized by collisions or electric and magnetic fields. As a result of this longevity and the abundance of hydrogen it is particularly common for astronomers to observe radiation from the heavens at a frequency of 2.4GHz, now known to correspond to the hydrogen $n = 109$ to $n = 108$ transition [1]; such a highly excited hydrogen atom anywhere on Earth would be ionised almost immediately as the binding energy would be significantly below thermal energies. $Binding\ energy : E_B(n = 109) \sim 10^{-22}J, \quad thermal\ energy : E(T = 300K) \sim 10^{-20}J.$

1.2 The heavy Rydberg 'atom'

The heavy Rydberg 'atom' is not really an atom, rather it is an ionically bonded molecule; the term derives from the fact that they share many properties with conventional Rydberg atoms, and will be used throughout this report.

1.2.1 What is a heavy Rydberg atom?

Heavy Rydberg atoms consist of a positive and a negative ion orbiting each other in a bound system. Such a system can be treated as analogous to a highly excited hydrogenic nucleus/electron system as the energies of the two systems have the same dependence on the separation of the two bodies; leading to many similar characteristics.

The most commonly studied heavy Rydberg atom is the H^+/H^- system, consisting of a proton bound to a H^- ion. The H^- ion is simply a hydrogen atom with an added electron; as the single electron in a hydrogen atom cannot fully shield the nucleus from its environment, another electron brought into the same

region will feel an attractive force from the positive charge of the nucleus.

The H^+/H^- system was first detected in 2000 by a group from the University of Waterloo including my project tutor Dr Ralph Shiell. The discovery came from the development of a new technique called *threshold ion-pair production spectroscopy* [3] in which dissociation by an electric field is used to determine the threshold energy of dissociation for a given system

$$XY(q) \longrightarrow X^+(q'_X) + Y^-(q'_Y)$$

where q and $q'_{X,Y}$ represent the initial and final states respectively.

Heavy Rydberg systems containing various atoms have now been created, although the literature on the subject is sparse. Dr Shiell is now working on production of a Li^+/Li^- heavy Rydberg atom, the first such system composed of an alkali metal.

1.2.2 What makes heavy Rydberg atoms interesting?

Since their recent discovery, heavy Rydberg atoms have been increasingly used in experimental atomic/molecular physics; their relatively large reduced mass, leads to a very slow time evolution, which makes them easy to manipulate both spatially and energetically, while their low binding energy makes them relatively simple to detect through field dissociation and detection of the resulting ions.

Kepler's third law states that the period of an orbit is proportional to the cube of the semi-major axis; this can be applied to the Coulomb force

$$\tau^2 = \frac{4\pi^2\mu}{kZe^2}a^3 \tag{1.7}$$

where τ is the time-period, μ is the reduced mass and a is the semi-major axis [4].

Classically we can say that a system with a large reduced mass has a long orbital period. Quantum mechanically, a large reduced mass in a system leads to narrow spacing of the energy levels and the rate of time-evolution of the wavefunction depends on this energy spacing.

There is a relatively small quantity of literature on the subject of heavy Rydberg

atoms, the next three chapters contain discussion and analysis of results from a dynamic simulation of both conventional and heavy Rydberg atoms.

1.3 The structure of this report

Having given an overview of the general properties that make Rydberg systems an interesting topic of study, the next two chapters focus on the contruction of a set of numerical simulations as tools for investigating these properties further.

Chapters 4 & 5 examine the classical and quantum mechanical interpretations of the Stark effect respectively.

In chapter 6 I attempt an analytical solution of the classical equations of motion on which the simulation is based.

Chapter 7 examines the Runge-Lenz vector as a tool for determining the properties of orbits and a particular generalisation of the Runge-Lenz vector that remains constant around the orbit even with the application of an external electric field.

Finally chapter 8 demonstrates the extension of the simulation to three dimensions.

The report ends with conclusions and appendices providing derivations and the code for the various MATLAB simulations.

Chapter 2

Constructing the Simulation

A numerical simulation was constructed to model the behaviour of different Rydberg systems subjected to a static external electric field. After consultation with various people, the decision was made to use MATLAB, due to its general suitability and its availability within the University.

The two initial versions of the simulation model a hydrogen atom in a highly excited state and a simple heavy Rydberg system (H^+/H^-), with motion confined to a plane. Later in the project the simulation is extended to cover the alkali metals, other heavy Rydberg systems with a more asymmetric mass distribution and all extended into three dimensions.

2.1 Constructing the simulation: no electric field

For the simulation to remain physically realistic, it has to demonstrate conservation of both energy and angular momentum. As it is based on a numerical integration algorithm we expect to accumulate small errors at each timestep, so it is important that the accumulated error after running the simulation remains small.

The first version was based on Euler's numerical integration algorithm and used the constant acceleration formulae to calculate new positions and velocities from the values at the last timestep. This model fell at the first hurdle, with total energy and angular momentum increasing in magnitude at each timestep.

The solution to the energy/momentum problem required the use of a differ-

ent algorithm. An excellent website[1], containing graphical simulations of simple spring-mass systems suggested using the 4th order Runge-Kutta algorithm (see appendix A). The great strength of this particular technique is its stability; even with a large integrating step-size it is able to produce a stable, bound orbit, with energy and angular momentum conserved except for a small numerical integration error proportional to h^5, where h is the stepsize.

2.1.1 The hydrogen atom

Based on our new definition of the Rydberg state, introduced at the beginning of chapter 1, as a state in which the outer electron feels a hydrogenic potential, it is clear that all states of hydrogen can be treated as Rydberg states; the first simulation models the hydrogen atom to allow comparison with the behaviour of other atoms in Rydberg states.

The potential within a hydrogen atom is geometrically identical to a planetary, gravitational potential. This correspondence with a well understood, essentially classical system, gives confidence that the main properties of the hydrogen atom can be reproduced in a classical simulation. The extention of the simulation to cover more complex Rydberg atoms should allow testing of the ability of a classical model to reproduce quantum effects and demonstrate the correspondence principle linking classical and quantum mechanics.

The hydrogen atom is a two body system (proton + electron), however if the observer's frame of reference (from which measurements are taken) is coincident with the rest frame of the proton, we have a restricted two body problem that can be represented by a single particle with the proton taken to be fixed at the origin. This approach can greatly simplify a dynamic problem such as this, at the expense of losing any information about the position and velocity of the centre of mass.

It is important to remember that the presence of the nucleus is represented only by its potential well, the program itself doesn't 'know' that there is a mass at the origin.

The unique properties of the hydrogen atom that separate it from the other

[1] http://www.myphysicslab.com/

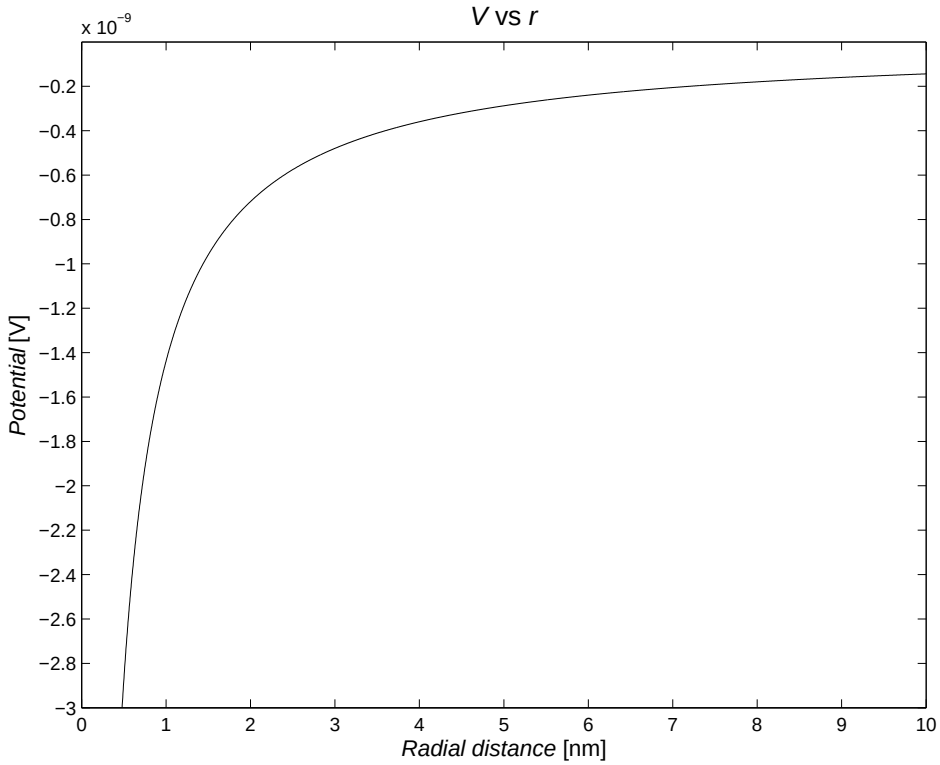

Figure 2.2: The hydrogen atom's unperturbed $1/r$ potential makes it an ideal candidate for investigating the effects of externally applied fields.

group I elements are mostly the result of its pure $1/r$ potential with no correction terms (see figure 2.2). This perfect symmetry comes from a nucleus consisting of a single proton which therefore cannot be polarised[2] and has no inner shells of electrons to provide natural boundaries between regions with a different form for the potential.

2.1.2 The heavy Rydberg 'atom' in the lab frame

When approaching the simulation of a system of two bodies (A & B) of comparable mass, it seems natural to dissociate the observer's frame from either body, as there is no reason to favour one over the other. This led me to construct this second simulation with separate positions and velocities measured relative to an origin fixed in space. While this nearly doubled the number of variables required, it also made the simulation more general as the reduced mass particle model is not

[2]While the proton is thought to have a permanent electric dipole moment, the dipole field due to polarisation of the quark charges is negligible.

universally applicable. Transforming to a reference frame fixed in space can also give information on the position and velocity of the centre of mass of the system.

The separation of the observer's frame of reference from either body changes the way that the potential is calculated, as the separation of the charges depends not on the distance of a single particle from the origin:

$$r = \sqrt{x^2 + y^2} \tag{2.1}$$

but on the separation of the two bodies:

$$R = \sqrt{(x_A - x_B)^2 + (y_A - y_B)^2}. \tag{2.2}$$

A further complication arises in calculation of the total energy of the system and the individual energies of the two particles. It is informative to calculate separate kinetic energies for each component of the system, however potential energy is only defined for the system as a whole (a single, isolated charge has no potential energy); this makes it very difficult to calculate a meaningful value for the total energy of an individual component.

2.1.3 The reduced mass particle model

The same single particle technique used to simulate the hydrogen atom in section 2.1.1 can be applied to the heavy Rydberg system, the major difference being the relative masses of the two particles; in this first heavy Rydberg simulation the two components will be assumed to have equal mass.

The most commonly studied heavy Rydberg atom is the H^+/H^- system, consisting of a proton bound to a H^- ion, which can be treated as a system of two opposite charges of equal mass (the difference in mass $\approx 0.015m_p$). As the two components of the system are of comparable mass, extra care must be taken in converting to the single particle formulation of the problem.

For two particles with masses $m_1 \& m_2$ the corresponding single particle has mass given by

$$\mu = \frac{m_1 m_2}{m_1 + m_2}. \tag{2.3}$$

For the initial versions of the simulations we concentrate on two special cases. Hydrogen atom: $m_1 = m_p$, $m_2 = m_e$,

$$m_p \gg m_e \Rightarrow \mu \approx m_e.$$

Heavy Rydberg H^+/H^- system: $m_1 \approx m_2 \approx m_p$,

$$\Rightarrow \mu \approx \frac{m_p}{2}.$$

We now have simulations for both types of Rydberg system in the same *'reduced mass, single particle'* form; this should facilitate direct comparisons of their properties.

2.2 Constructing the simulation: application of an electric field

The addition of an external electric field essentially makes this a restricted three-body problem, with interactions between two particles and an electric field, all confined to a plane. Figure 2.3 shows the geometry of the potential along the x-axis for a Rydberg atom in an external electric field.

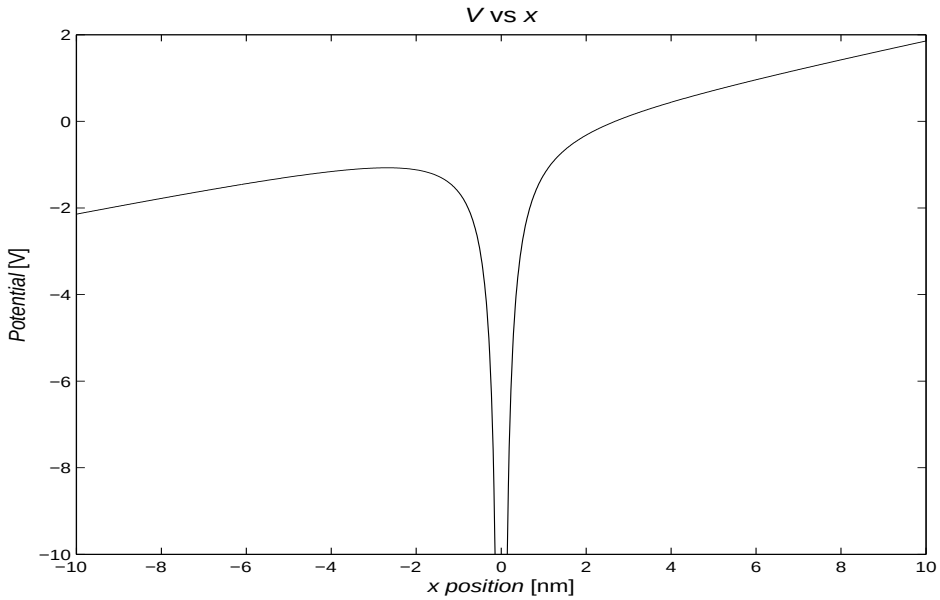

Figure 2.3: Combined Coulomb-Stark potential along the x-axis for a field of $3 \times 10^6\ Vm^{-1}\hat{x}$.

2.2.1 The hydrogen atom

Initially choosing starting conditions to give the electron a circular orbit of radius 3nm in the $x-y$ plane, a static electric field was added ($\vec{E} = 3 \times 10^6 V m^{-1} \hat{x}$). The interaction of the electric field with the charge on the electron has the effect of reducing the angular momentum of the orbit, causing the electron to follow a more elliptical path and bringing the perigee of the orbit ever closer to the nucleus. As it approaches the centre of the $1/r$ potential, the velocity increases dramatically, rapidly increasing the distance travelled at each timestep and effectively reducing the resolution of the simulation.

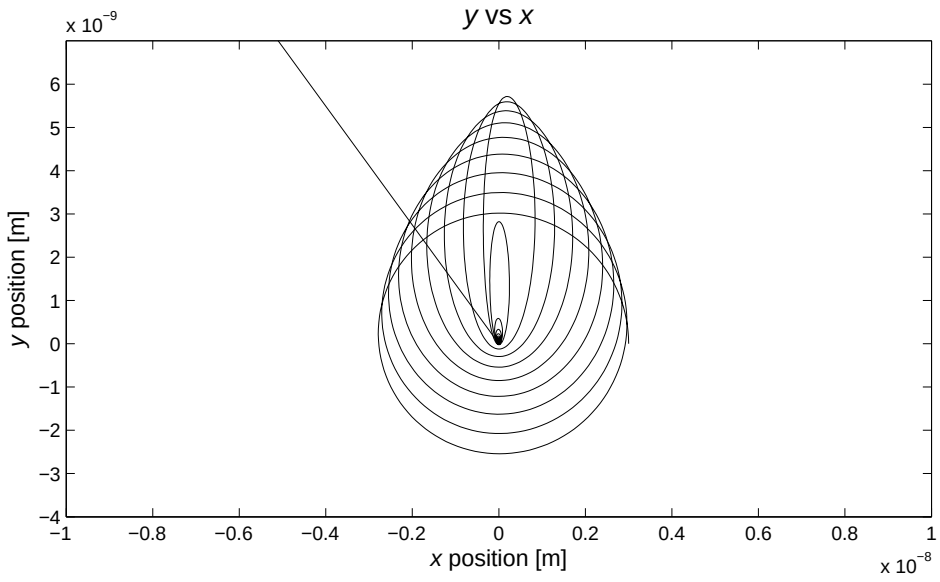

Figure 2.4: At low values of r the resolution of the simulation is insufficient to produce a stable orbit.

When very close to the nucleus, the low resolution of the simulation means that inaccuracies in the numerical integration algorithm cause the electron to pass through (or at least very close to) the nucleus and experience an excessively large force. Figure 2.4 shows the trajectory of the electron as it first experiences a small pertubation to the orbit and then is ejected from the atom entirely.

The presence of a $1/r$ potential at the origin, produces an effective *"singularity"* at the centre. Figure 2.5 shows that the total energy of the system remains

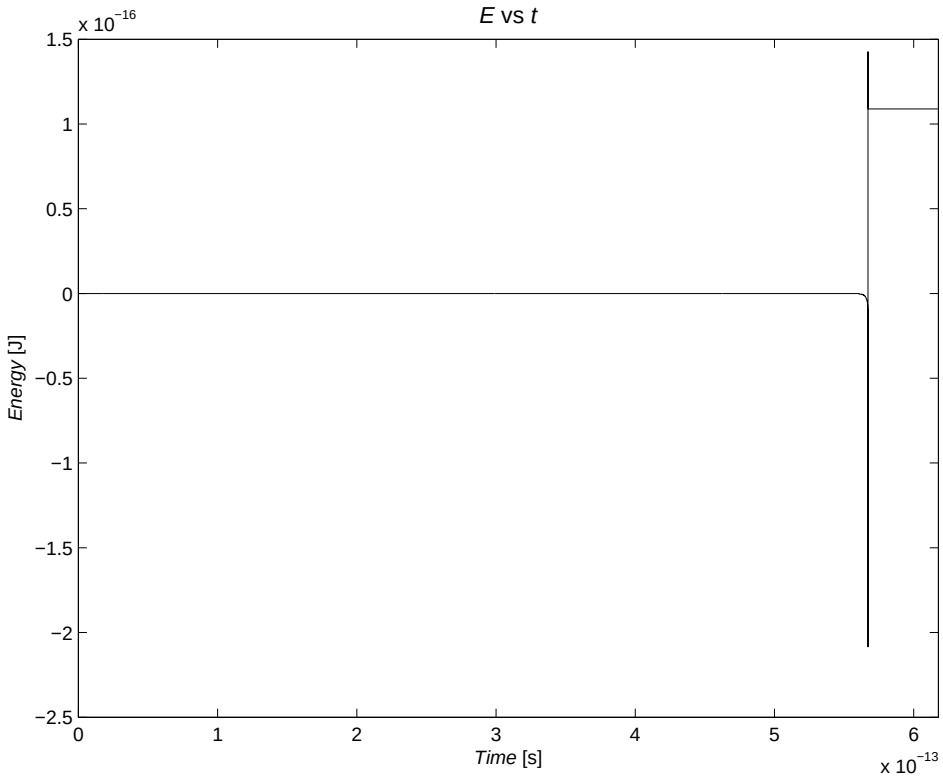

Figure 2.5: Energy is not conserved due to interaction with singularity.

conserved until the first interaction with the 'singularity', at which point a small pertubation reduces the energy slightly, just before the second interaction causes the electron to be ejected from the atom completely.

Although the laws of physics demand that the total energy of a closed system is always constant, numerical inaccuracies in the integration algorithm cause the electron to pass through the nucleus. Note that once the electron is out of the immediate vicinity of the nucleus the energy remains constant, as expected.

2.2.2 The heavy Rydberg atom

The same problem exists in the simulation of the heavy Rydberg atom (see figure 2.6); as the two ions are oppositely charged, a 'collision' (or rather *extremely* close encounter) causes them to feel very large forces in opposite directions, leading to the disintegration of the system.

The electric field applied to the heavy Rydberg atom in figure 2.6 is the same magnitude as that applied to the conventional Rydberg atom in figure 2.4. The

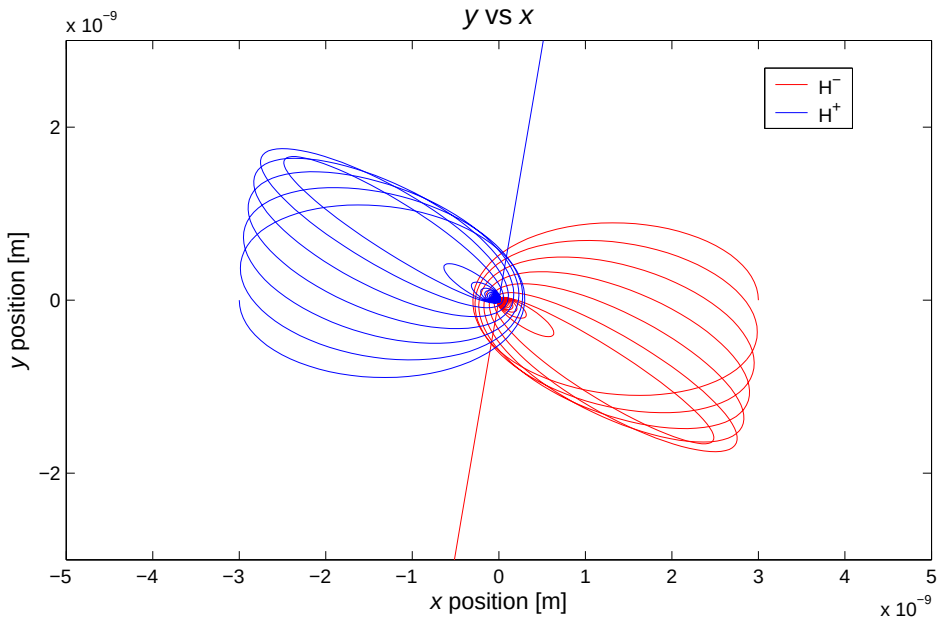

Figure 2.6: "Collision" of oppositely charged ions leads to disintegration of heavy Rydberg system.

momentum of the two systems is of a similar magnitude and so they show a similar response to the applied field, even though the mass of the heavy Rydberg system is much larger and the relative velocity of the components of the conventional Rydberg atom is two orders of magnitude higher.

2.3 Adaptive stepsize

Various solutions to the 'singularity' problem were considered, mainly based around the idea of introducing an additional term to prevent the force from tending to infinity at the centre (the 'bouncy proton' solution), however they all seemed fairly contrived, without any physical justification.

The real problem wasn't the form of the equations, but in the inaccuracies inherent in numerical integration. These combined with the reduced resolution when the separation of the opposite charges is small, cause the close encounters that break up the system. In order to improve the resolution of the simulation at small separations, I decided to use an adaptive stepsize of the form:

$$h_n = \left(\frac{r_{n-1}}{r_0}\right)^m h_0 \tag{2.4}$$

where:

$$t_n = t_{n-1} + h_n \tag{2.5}$$

and m can be chosen to give the required resolution; $m = 2$ has proved sufficient for all conditions encountered in simulating the hydrogen atom and the H^+/H^- heavy Rydberg system. Later simulations of more complex systems required $m = 3$, see section 3.1.1.

2.4 Initial results

The use of the 4th order Runge-Kutta algorithm with an adaptive stepsize solved the singularity problem by increasing the spatial resolution and did not require the addition of non-physical terms.

The trajectory of a component of the heavy Rydberg system is very similar to that of the electron in a hydrogen atom. This is due to the hydrogenic potential centred about each ion.

Figure 2.7 shows the response of the electron in a hydrogen atom to an applied field, while figure 2.9 shows the response of the H^+/H^- system to the application of an identical field. Figure 2.8 demonstrates conservation of energy in the hydrogen atom simulation.

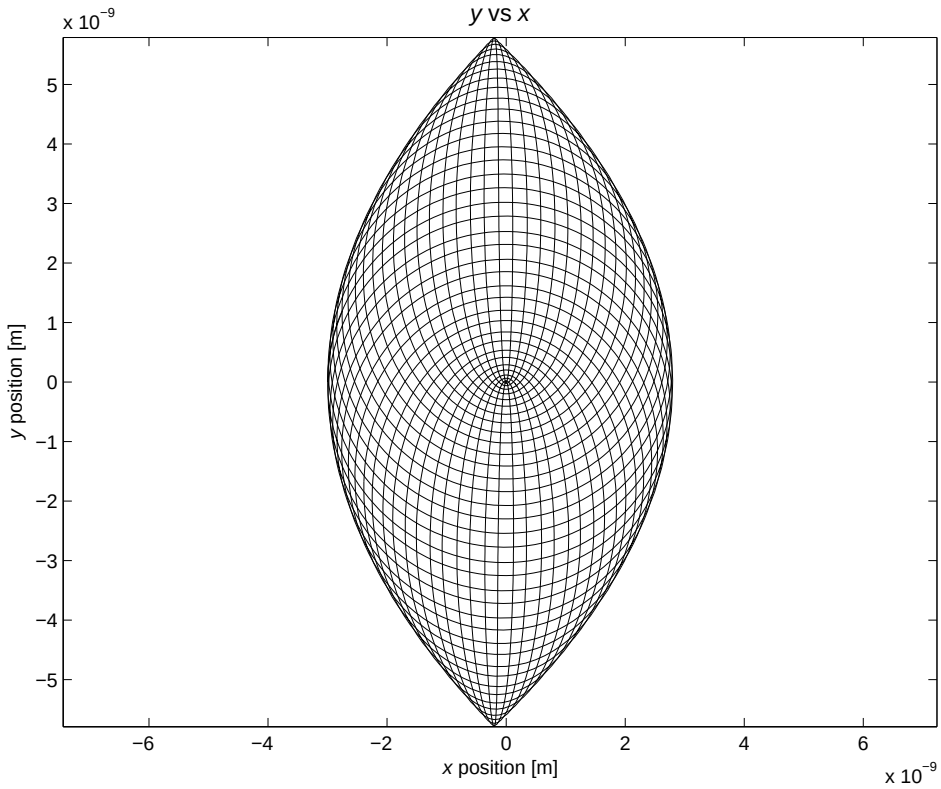

Figure 2.7: Trajectory of the electron in a hydrogen atom, on an initially circular orbit, subjected to an electric field $\vec{E} = 3 \times 10^6 V m^{-1} \hat{x}$.

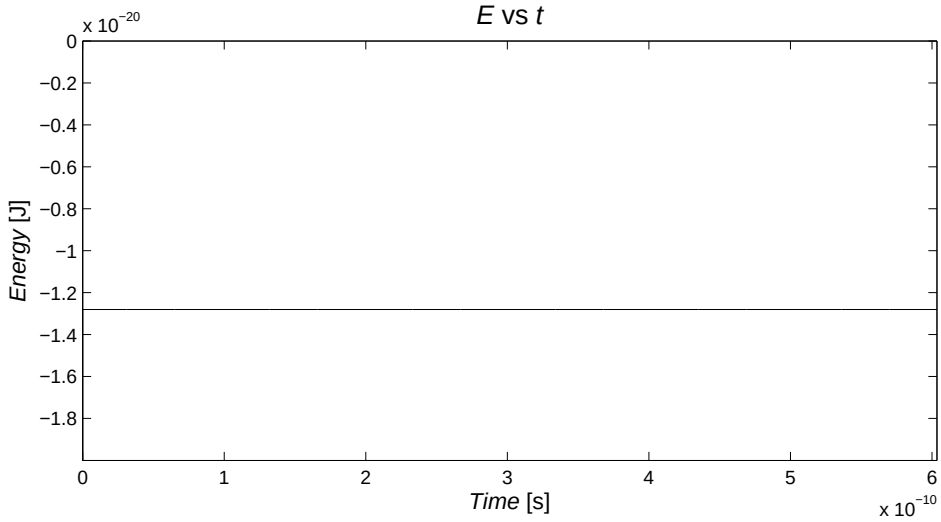

Figure 2.8: The addition of adaptive stepsize made the simulation robust enough to reproduce a stable orbit even when passing close to the nucleus. Energy is conserved.

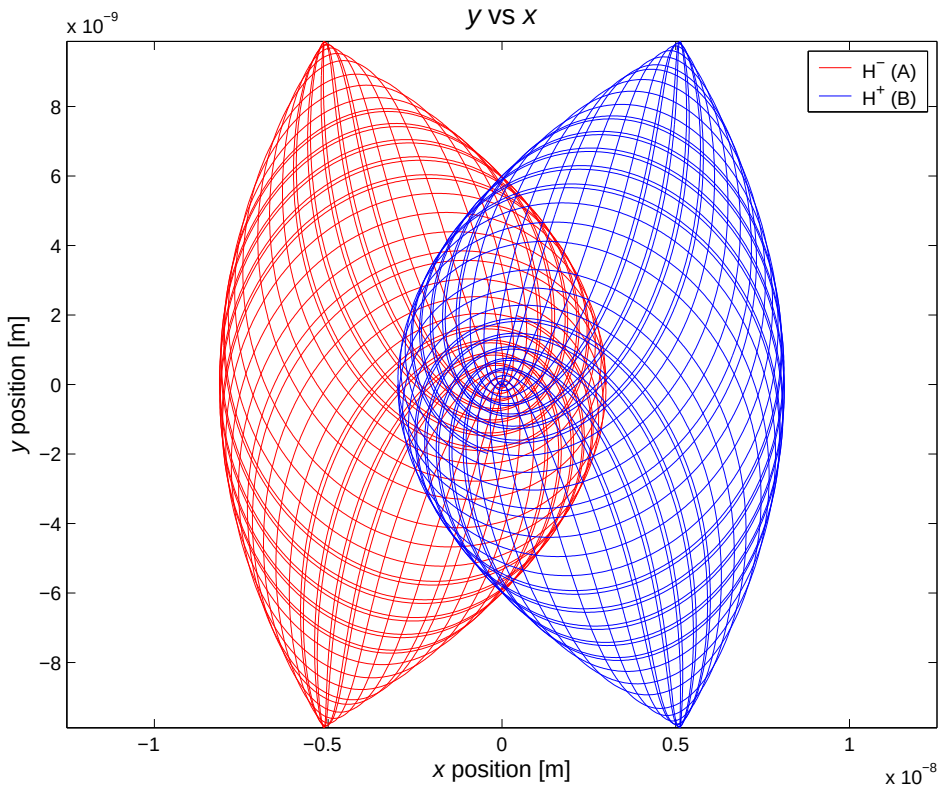

Figure 2.9: Trajectories of the two bodies in a H^+/H^- heavy Rydberg system subjected to an electric field $\vec{E} = 3 \times 10^6 V m^{-1} \hat{z}$.

Chapter 3

Extending the simulation

3.1 Conventional Rydberg atoms

All of the conventional Rydberg atom results presented in this report so far have applied only to the hydrogen atom. To extend the MATLAB code to simulate other atoms, extra terms had to be inserted into the equations of motion to account for the effects on the outer valence electron of penetrating the inner electron shells.

3.1.1 The potential within the ion core

To obtain the form of the potential within the ion core without an external field, we start with Gauss' law

$$\oint \vec{E}.d\vec{A} = \frac{Q}{\varepsilon_0} \tag{3.1}$$

When passing close to the nucleus, the valence electron feels the full charge of $+Ze$; as it moves outwards the effective charge decreases as the positive charge of the nucleus is shielded by the inner electrons.

$$Q_E(r) = Ze - (Z-1)e\frac{r^3}{R^3} \tag{3.2}$$

where $R \equiv$ radius of the ion core.

This assumes that the electron charge is evenly distributed inside the core.

Choosing a spherical Gaussian surface of radius r and then Substituting the effec-

tive charge into equation 3.1, we can calculate the electric field inside the core

$$\vec{E}(r < R) = \left[\frac{kZe}{r^2} - \frac{k(Z-1)er}{R^3}\right]\hat{r}. \tag{3.3}$$

The electric field is related to the potential by

$$E = -\frac{dV}{dr} \tag{3.4}$$

which gives the potential within the ion core

$$V(r < R) = \frac{kZe}{r} - \frac{k(Z-1)e}{2R} - \frac{k(Z-1)er^2}{2R^3}. \tag{3.5}$$

Outside the core the nucleus is shielded by $Z-1$ electrons and has an effective charge of $+e$ no matter what the charge of the nucleus.

The increased complexity of this version of the simulation required a change in the form of the adaptive step-size ($m = 3$, see section 2.3).

3.1.2 Precession

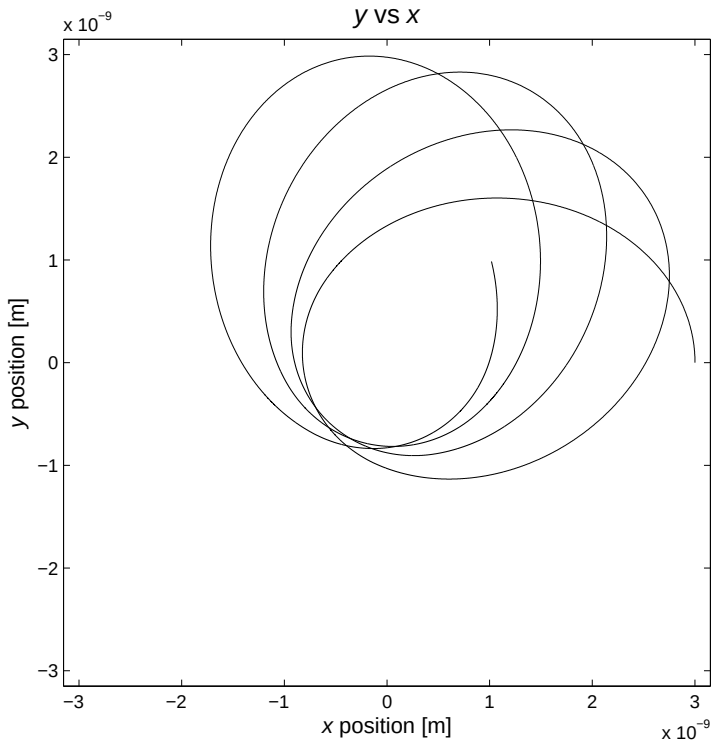

Figure 3.1: Deviation from a $1/r$ potential causes precession of the orbit.

A particle orbiting in a hydrogenic, $1/r$ potential follows a closed, elliptical orbit radially bounded by r_{min} & r_{max}. Once the outer electron penetrates the ion core, the gradient of the potential becomes steeper exerting a larger force, with the largest force exerted at the perigee. As a result of this additional force the orbit does not return to its initial position at $r = r_{max}$; the change in angular position between successive values of r_{max} is known as precession (see figure 3.1).

In chapter 1 we looked at exceptions to the definition of Rydberg atoms as atoms with hydrogenic potentials. This is a good example of such an exception; the behaviour demonstrated here is significantly different from the hydrogen results shown in chapter 2. This gives a good demonstration of the reason for defining Rydberg atoms as we have; in a higher energy state the outer electron would spend less time inside the ion core and the angular separation between successive values of r_{max} would decrease. Once a sufficiently high value of n is reached we would expect negligible precession (low values of l can be interpreted as extremely eccentric orbits which may still penetrate the inner electron shells).

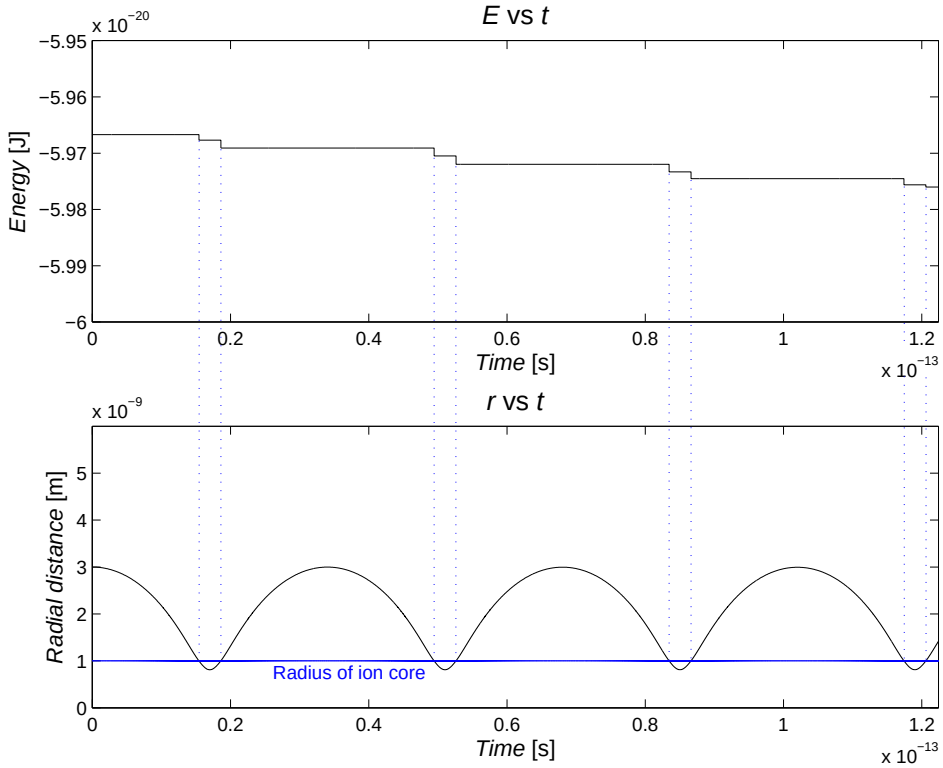

Figure 3.2: The discontinuous force across the boundary of the ion core causes a jump in the energy of the system.

There remains a problem with the energy when crossing the boundary between the two different forms of the potential. When crossing the barrier, the potential is continuous, however the force is not continuous but has a sudden increase in magnitude when passing inside the boundary. Figure 3.2 shows how the total energy, conserved within either region, makes a small, discrete drop when passing from one region to another. Decreasing the step-size reduces the magnitude of this drop.

3.2 Heavy Rydberg atoms

In this section we will consider the extension of the simulation to cover heavy Rydberg atoms with two ions of comparable but unequal mass.

3.2.1 The $fluorine^- - hydrogen^+$ system

The heavy Rydberg plots in chapter 2 demonstrate a perfect symmetry (see plots 2.6 & 2.9); if the complete trajectory of one ion was reflected through the origin, it would superimpose perfectly over the trajectory of the other ion. This is due to the identical masses and opposite starting positions and velocities relative to an origin placed at the system's centre of mass.

We now examine the case where a proton is bound with an F^- ion (a fluorine atom Z = 9, with a single electron added). While fluorine has a higher atomic number than hydrogen, this heavy Rydberg system still conforms to our working definition discussed in chapters 1 & 2. As both the fluorine and the hydrogen are significantly more compact than their orbital separation, the hydrogen *sees* the fluorine as a charge of $+1e$ while the fluorine *sees* the hydrogen as a charge of $-1e$.

The mass of fluorine is significantly higher than that of hydrogen ($m_F \approx 19m_H$); adjusting the original heavy Rydberg atom simulation to cover this new situation was simply a matter of changing the mass in the equations of motion. The original simulation has separate equations of motion for the H^+ and F^- ions, so this requires no restructuring of the model; the masses m_H & m_F are inserted into the initial list of constants (see figure 3.3).

From our updated simulation we can extract data on the variables: R_x & R_y,

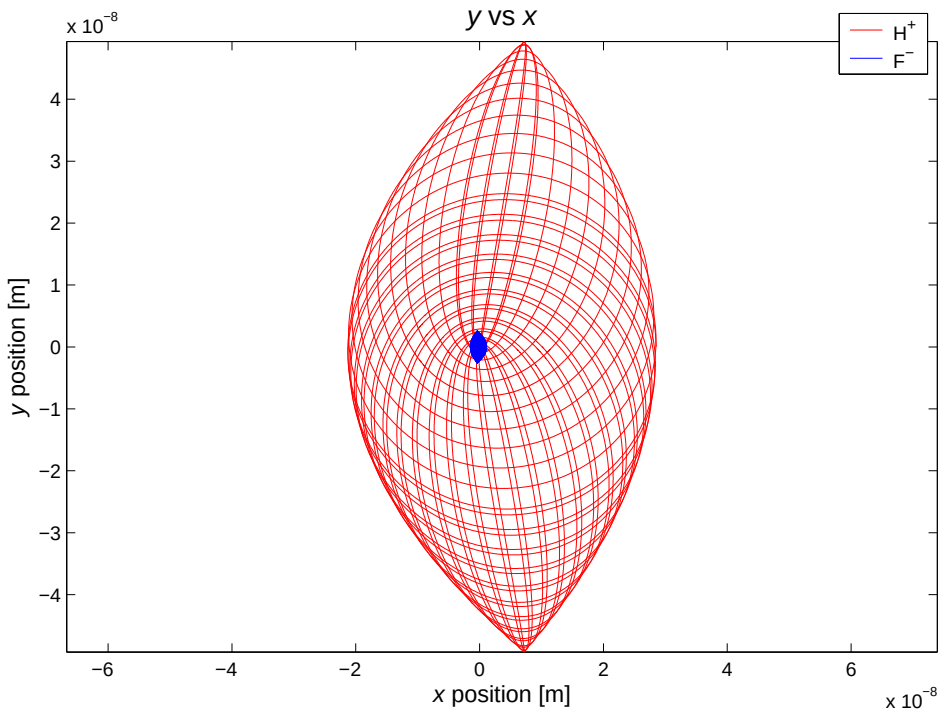

Figure 3.3: The two trajectories shown are identical if reflected through the origin and scaled by a factor of 19.

which measure the x & y components of the *separation* of the two ions. If the reduced mass particle model remains valid in these conditions then plots of this data should be identical to the x/y plots showing the trajectory of the corresponding reduced mass particle.

A single particle representing the F^-/H^+ system would have mass given by

$$\mu = \frac{m_F m_H}{m_F + m_H} \quad \Rightarrow \quad \mu \approx \frac{19 m_H^2}{20 m_H} \tag{3.6}$$

which gives a particle mass $\mu \approx \frac{19}{20} m_H = 1.59 \times 10^{-27} kg$.

Figure 3.4 is a plot of the x & y *separations* of the hydrogen and the fluorine. It gives a clear demonstration of validity of the comparison between heavy and conventional Rydberg atoms; whatever the total mass of the system, however that mass is distributed, if the separation of charges is large then the potential will be effectively hydrogenic, resulting in behaviour similar to that of the hydrogen atom.

A major difference between this simulation and that of hydrogen is that our

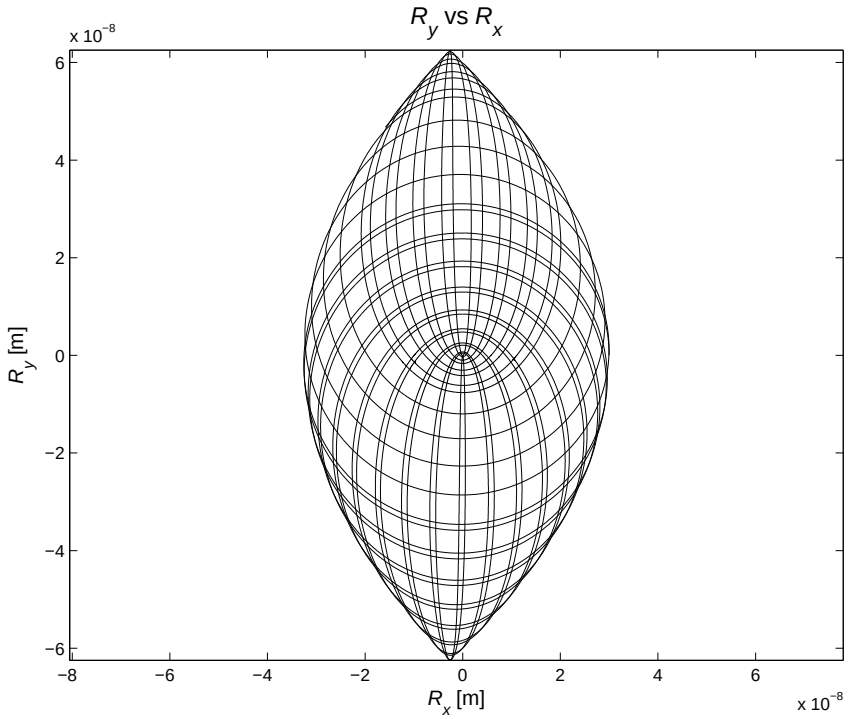

Figure 3.4: The H^+/F^- heavy Rydberg system displays similar behaviour to the hydrogen atom.

reference frame is now fixed in space which allows us to plot the individual trajectories of the two bodies, independently of each other.

The extention of the simulations to model any general Rydberg atom and any two-body, heavy Rydberg system has demonstrated the similarity of the two types of system. The study of heavy Rydberg atoms is still in its infancy; the results presented so far clearly demonstrate the link they provide between the well understood hydrogen atom and more complex atomic and molecular systems.

Chapter 4

Analysing the response to an electric field: the classical Stark Effect

The application of an external electric field (often known in atomic physics as a Stark field) has a dramatic effect on Rydberg atoms. While ground state atoms are largely unaffected by electric fields, Rydberg atoms with their large charge separations and corresponding large electric dipole moments and low binding energies, are perturbed and can even be ionised by a relatively weak field.

4.1 The conventional Rydberg atom

During the initial construction of the simulations, the key features I was trying to reproduce were conservation of energy and angular momentum. Energy is conserved within any closed system while angular momentum is only conserved in the absence of an applied torque; the simple $1/r$ potential centred about the nucleus never applies torque to the electrons, as the force is always anti-parallel to the position vector

$$\vec{\tau} = \vec{r} \times \vec{F} = |\vec{r}\,||\vec{F}| \sin\theta \tag{4.1}$$

$\theta = \pi \; rads \Rightarrow \tau = 0$, thus angular momentum is conserved

$$\frac{dL}{dt} = 0 \tag{4.2}$$

With the application of a constant electric field ($\vec{E} = 3 \times 10^6 \; Vm^{-1} \; \hat{x}$), the electron feels a continuously changing torque, which goes to zero as it crosses the x-axis. The resulting trajectory becomes progressively more distorted over time, eventually going through the full range of angular momentum from $[\vec{L} = L_{MAX}\hat{z}]$, to a straight line $[\vec{L} = 0]$, to the initial orbit in the opposite sense $[\vec{L} = -L_{MAX}\hat{z}]$.

Figure 4.1 shows the trajectory through one complete cycle of the angular momentum.

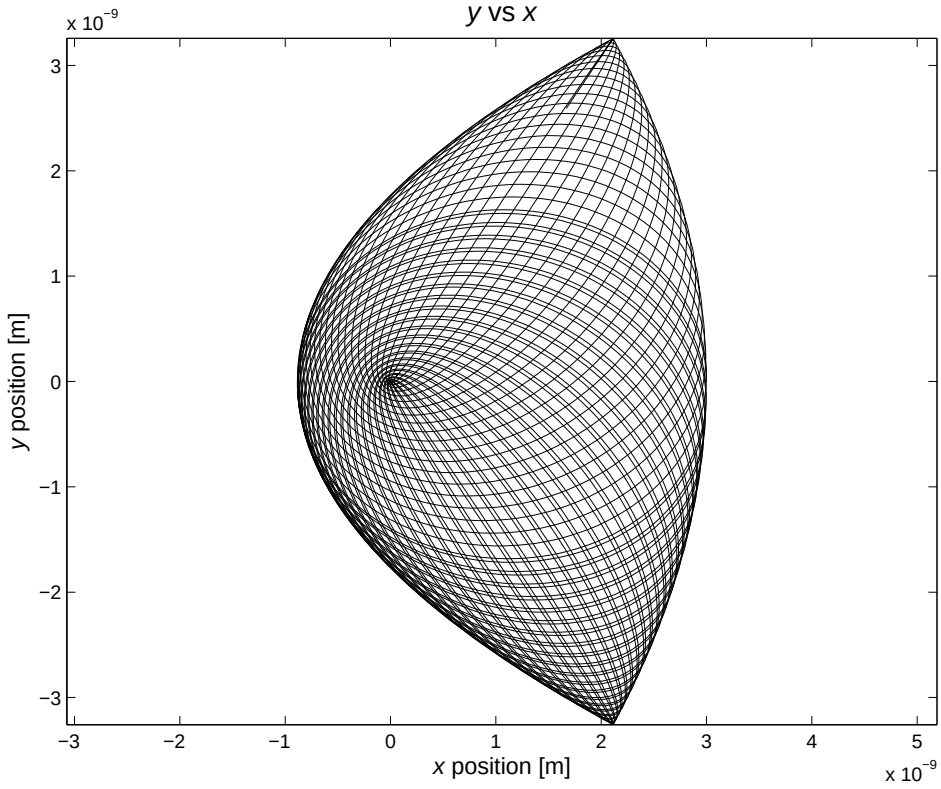

Figure 4.1: Trajectory of the electron in a hydrogen atom, initial orbital eccentricity $\epsilon = 0.522$, subjected to an electric field $\vec{E} = 3 \times 10^6 Vm^{-1}\hat{x}$.

4.1.1 Analysing the orbital angular momentum

There are two different effects that cause the angular momentum to oscillate: when the electron is moving upfield, it feels an acceleration incresing its speed and the angular momentum is increased, when the electron is moving downfield it feels a deceleration, decreasing its speed and the angular momentum is decreased. This effect results in a relatively small oscillation with a time-period determined by the period of successive circuits around the nucleus.

There is a feedback effect, due to the distortion of the the orbit by this small oscillation. Over time the amplitude of the oscillation in the x-component of the position of the electron decreases; this causes the orbit to becomes more elliptical (decreasing angular momentum) as the y-component is unaffected by the presence of the field.

Figure 4.2 shows the resultant angular momentum, which is the sum of two oscillating functions of different frequencies

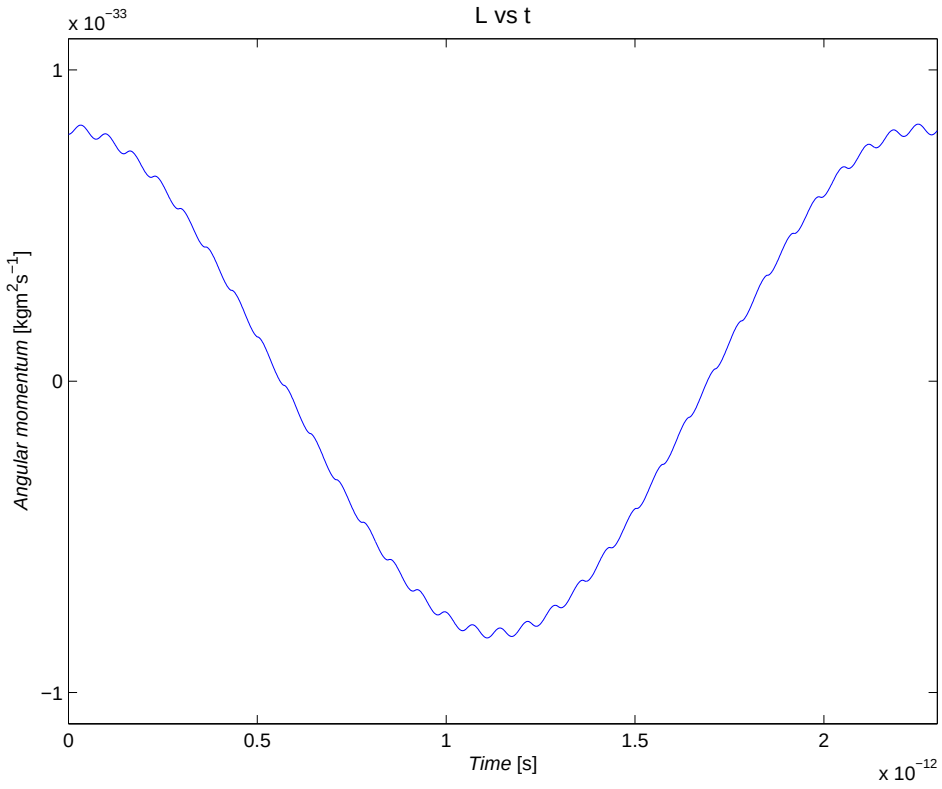

Figure 4.2: Oscillating angular momentum in a hydrogen atom, due to interaction with a Stark field.

Determining the period of oscillation

While the time-period of the high frequency component is simply the period of successive circuits about the nucleus, the factors determining the period of the low frequency oscillation are by no means obvious and required further investigation.

As angular momentum is conserved in the absence of the Stark field, it seemed likely that the period of any cyclical changes must depend on the field strength. From the simulation I extracted data relating the time-period of the low frequency oscillation in angular momentum to the electric field strength, with all other parameters kept constant. The plot is shown in figure 4.3

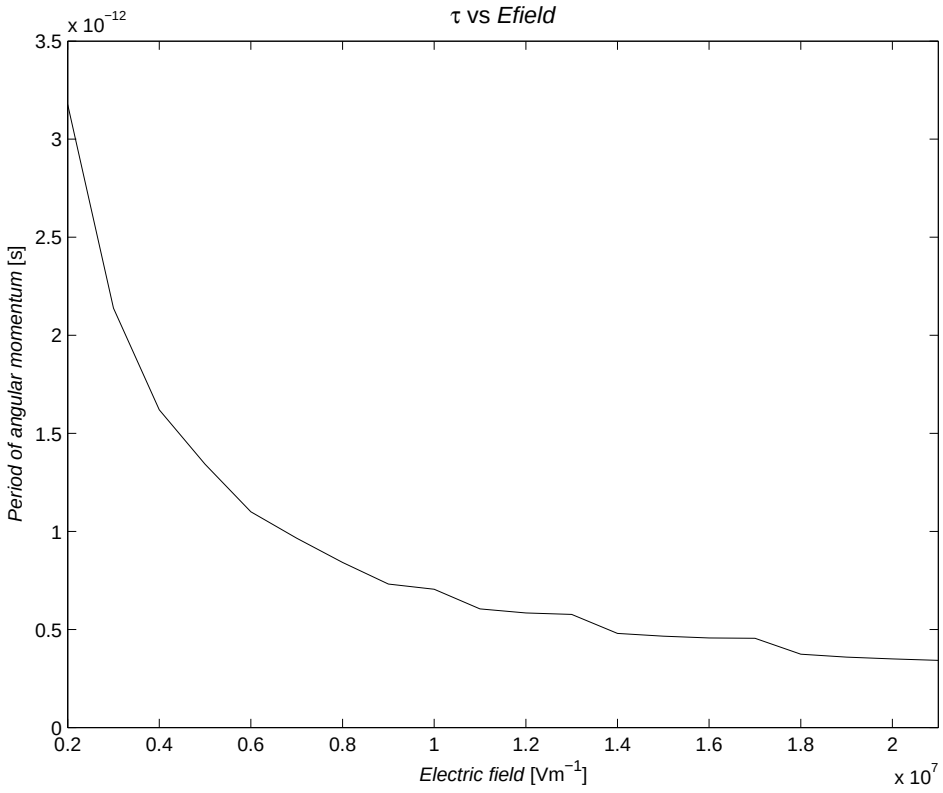

Figure 4.3: Dependence of angular momentum period on electric field strength.

Fitting the curve in figure 4.3 to various functional forms indicated a relationship:

$$\tau = C/E$$

where τ is the period, E is the electric field strength and C is a constant to be determined.

Investigating "C"

Calculating the numerical value of C was easy once the functional form had been determined. The first step was to input the data used to plot figure 4.3 into Excel; the solver function allows determination of the proportionality constant in an equation by minimising the differences between the data set and a set of trial values following the functional form expected of the actual data.

The numerical value obtained from Excel's solver function, combined with dimensional analysis, gives a value for C

$$C = 6.95 \times 10^{-6} V s m^{-1} \tag{4.3}$$

The next section of this chapter deals with the quantum mechanical view of the Stark effect and will present a derivation of C.

The form of the angular momentum

The angular momentum plot in figure 4.2 appears to take the form of a sum of two *cos* functions with different frequencies and amplitudes (the electron's motion is confined to the $x - y$ plane so $|L| = L_z$)

$$L = A_L cos(\omega_L t) - A_S cos(\omega_S t)$$

Using C to calculate the period of the long time-period oscillation, gives the angular frequency $\omega_L = \frac{2\pi}{\tau}$. The short time-period oscillation goes through 33 cycles for every one cycle of the long time-period oscillation, which allows us to calculate its angular frequency ω_S

$$\omega_L = 2.796 \times 10^{12} rad/s$$
$$\omega_S = 9.079 \times 10^{13} rad/s.$$

Using data giving the value of $\vec{L}$ at various times in the simulation, along with some trial and error, gives the long and short time-period amplitudes A_L & A_S

$$A_L = 8.094 \times 10^{-34} kgm^2 s^{-1}$$
$$A_S = 1.651 \times 10^{-35} kgm^2 s^{-1}.$$

A comparison of this model with the simulated angular momentum is shown in figure 4.4.

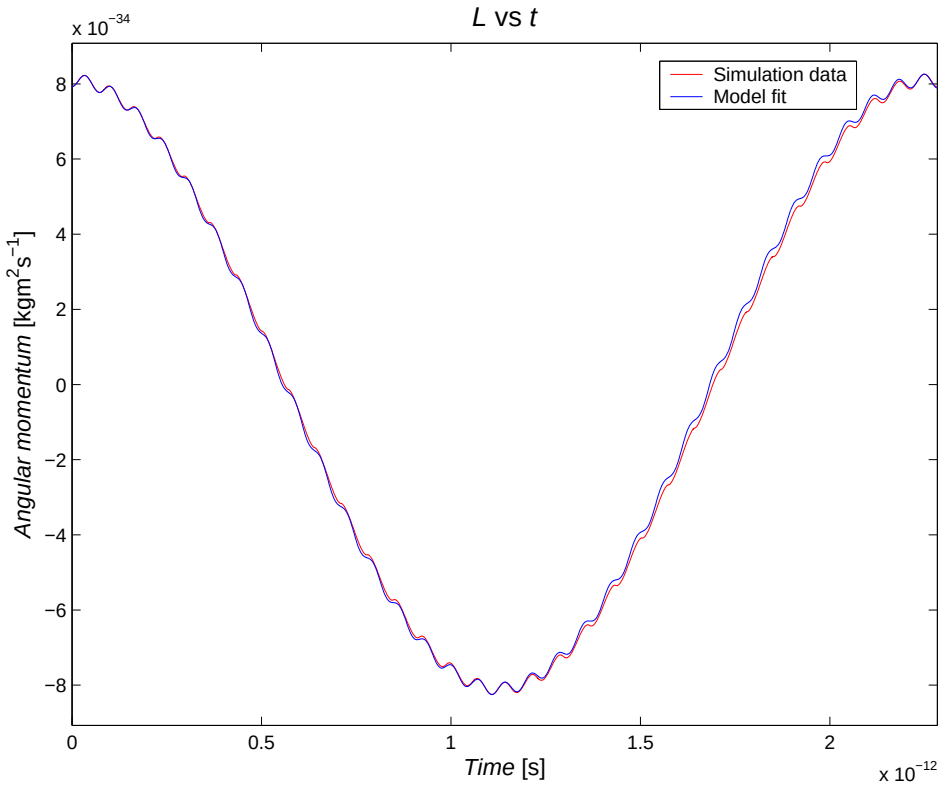

Figure 4.4: $L \approx 8.094 \times 10^{-34} cos(2.796 \times 10^{12} t) - 1.651 \times 10^{-35} cos(9.079 \times 10^{13} t)$ $kgm^2 s^{-1}$.

4.1.2 Ionizing effects

Due to their low binding energies, Rydberg atoms are particularly susceptible to ionisation by collisions, electric fields or transfer of kinetic energy from the ion core.

Field ionization

The saddle point on the combined Stark-Coulomb potential (see figure 2.3, $x = -2nm$) represents the classical ionisation limit. Starting from the form of the potential parallel to the electric field

$$V = \frac{ke}{|x|} + xE \tag{4.4}$$

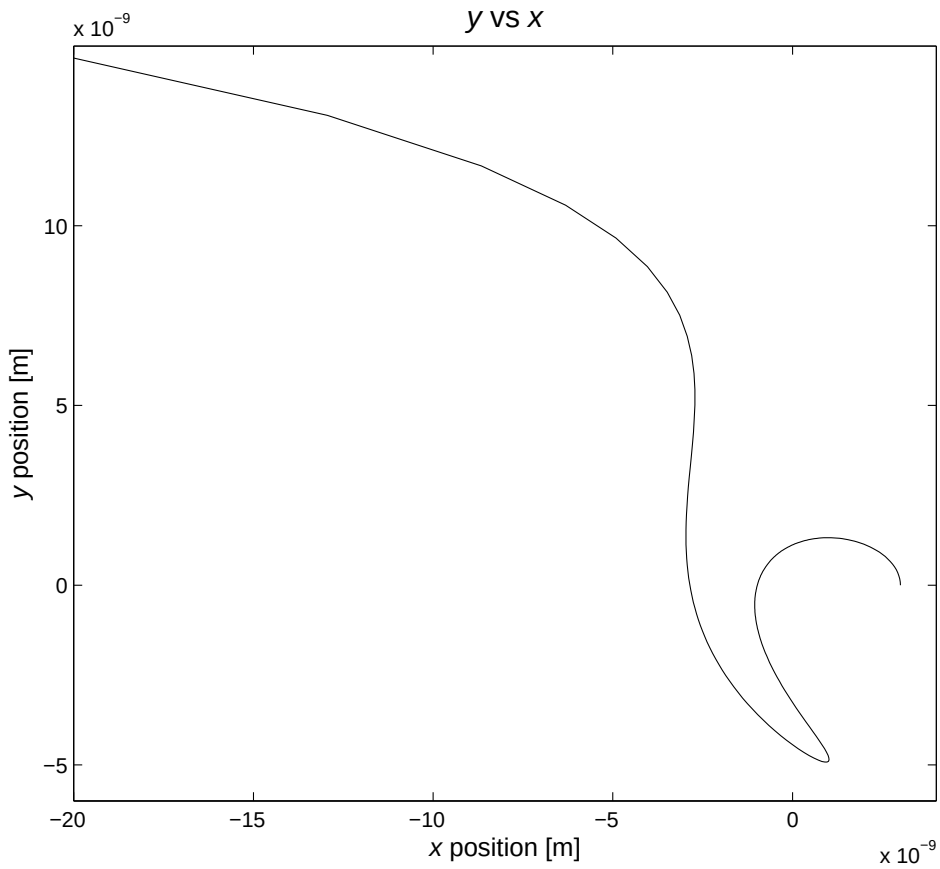

Figure 4.5: Simulated field ionisation of the hydrogen atom: $\vec{E} = 5.3 \times 10^7 V m^{-1} \hat{x}$.

where the electric field vector points in the positive x direction.

We now differentiate to find the stationary point

$$\frac{dV}{dx} = -\frac{ke}{x^2} + E = 0 \tag{4.5}$$

giving the position of the saddle point

$$x = \sqrt{\frac{ke}{E}} \tag{4.6}$$

for $E > 0$.

Substituting this into equation 4.4 gives the ionisation potential

$$V = -2\sqrt{keE} \tag{4.7}$$

which allows us to calculate the field strength needed to ionise an electron bound by energy W

$$E_c = \frac{W^2}{4ke^3}. \tag{4.8}$$

Entering the energy from the field free hydrogen simulation gives the classical ionisation field strength

$$W = -6.26 \times 10^{-20} J \quad \Rightarrow \quad E_c = 2.65 \times 10^7 V m^{-1}$$

Figure 4.5 demonstrates field ionisation of a hydrogen atom from the simulation. The required field strength was almost exactly twice the value calculated from equation 4.8, this is an interesting point which certainly requires further investigation, however time constraints will not allow it.

Autoionisation

Rydberg atoms often form in low pressure environments due to the combination of electrons and positive ions forming highly excited atoms. In this process the resulting atom can form with energy sufficient to raise outer electrons to the continuum where they are unbound.

4.2 The heavy Rydberg atom

The potential for each ion in a heavy Rydberg system is similar to that within a conventional Rydberg atom; they never feel a torque from each other as the force and position vectors are anti-parallel (see equation 4.1).

It is not suprising then, that the application of an electric field results in a similar response to that of the hydrogen atom and other Rydberg atoms; although the calculation of C is only valid for the hydrogen atom, the relationship between the period of the angular momentum and the electric field strength is probably of a similar form.

A comparison of the low and high field responses of the H^+/H^- system can be made looking at figures 4.6 & 4.8; a higher field results in greater spacing between successive circuits of the orbit. Figure 4.9 shows the H^+/H^- on an eccentric orbit in a strong field.

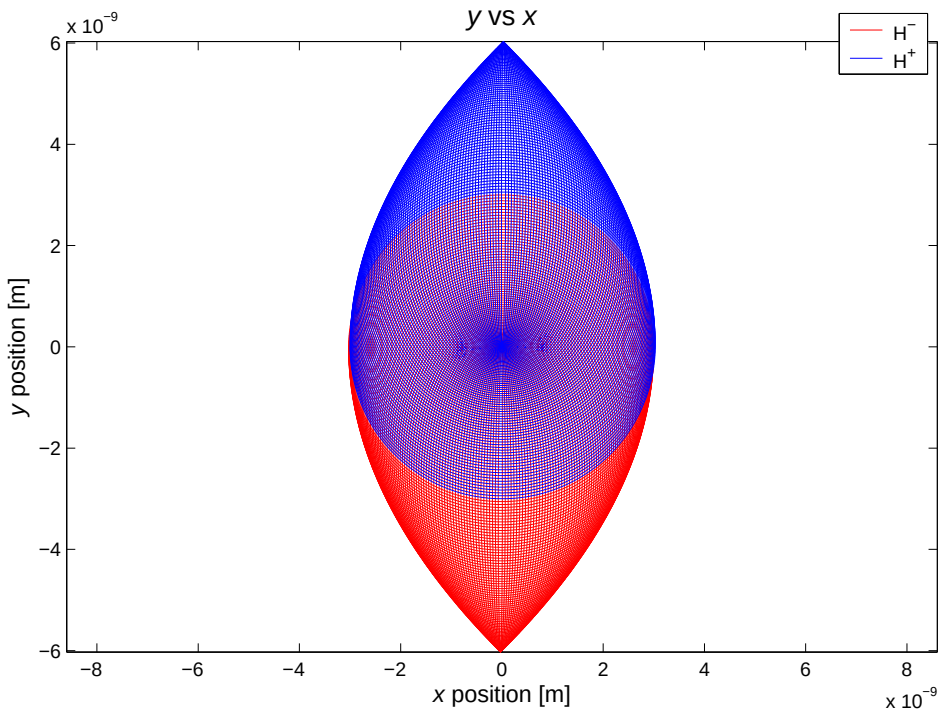

Figure 4.6: The H^+/H^- system on an initially circular orbit, in a weak electric field $\vec{E} = 4 \times 10^4 V m^{-1} \hat{x}$.

4.2.1 Field dissociation

The relatively low binding energy of heavy Rydberg atoms means that they are very sensitive to dissociation by electric fields; an effect analogous to field ionisation. This effect is used in the technique for determining the binding energy of heavy Rydberg systems, known as TIPPS (see section 1.2.1).

Figure 4.7 demonstrates field dissociation of a simulated H^+/H^- system.

4.3 Analysis of the orbital envelope

The envelope of an orbit refers to the outline of the shape produced when the trajectory of a particle is plotted through one full cycle of orbital angular momentum.

A high angular momentum, circular orbit produces an almost symmetrical envelope in both conventional and heavy Rydberg atoms (see figures 2.7 & 4.8), with the asymmetry introduced by the electric field vector pointing in the positive x direction.

For lower angular momentum, more elliptical orbits the envelope assumes a

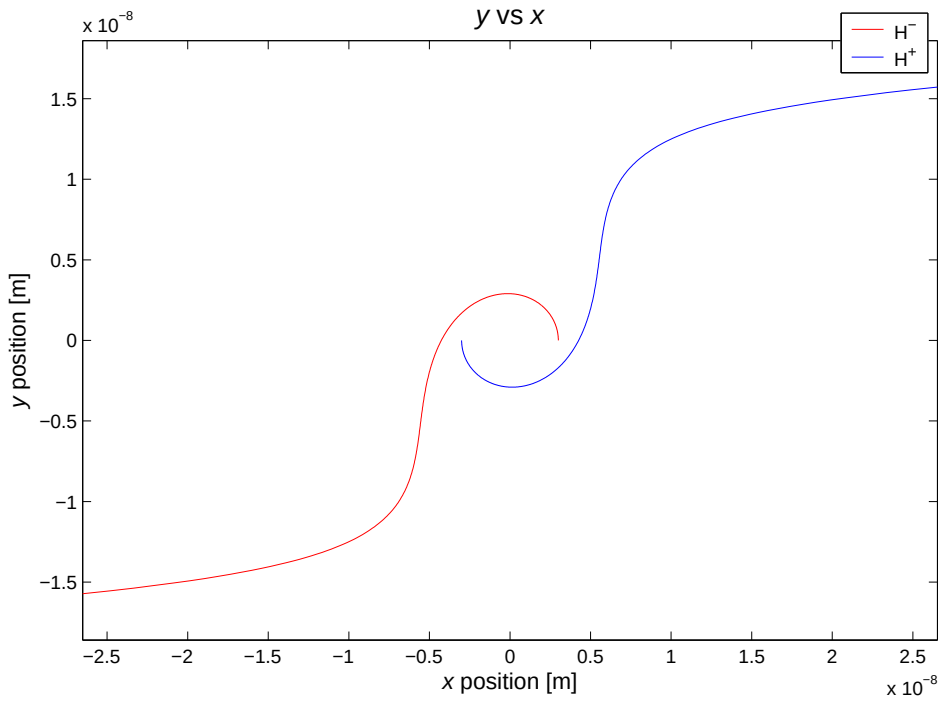

Figure 4.7: The simulated H^+/H^- system dissociated at $\vec{E} = 4 \times 10^6 V m^{-1} \hat{x}$.

distinctive 'butterfly' shape (see figures **??** & 4.9).

My initial reaction on seeing the original, high angular momentum plot in figure 2.7 was that the shape seemed well proportioned and generally aesthetically pleasing, the height being nearly, but not quite double the width. Closer inspection revealed that the major axis of the initial ellipse is the same length as the combined apogee and perigee (r_{max} & r_{min})

$$2a = \alpha + \beta \tag{4.9}$$

where a is the semi-major axis, α is the apogee and β is the perigee.
Comparisons with various plots of conventional and heavy Rydberg trajectories showed that this observation can be generalised to the statement:

"the length of the major axis of the ellipse formed by each successive circuit of the orbit is conserved for a given electric field strength."

Or expressed mathematically

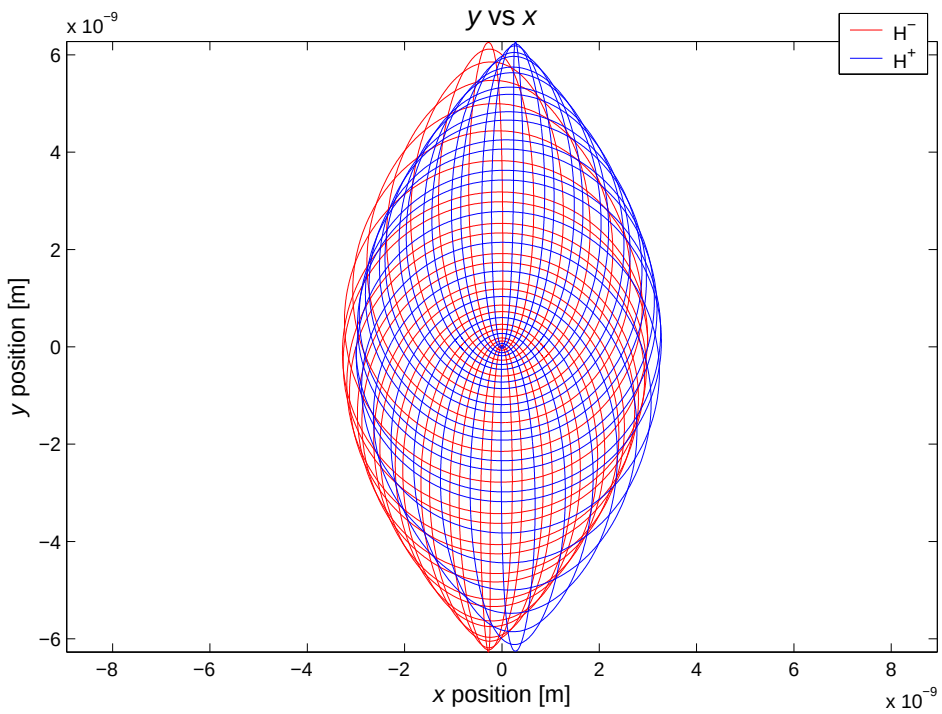

Figure 4.8: The H^+/H^- system, on an initially circular orbit, subjected to an electric field $\vec{E} = 8 \times 10^5 V m^{-1} \hat{x}$, through one full cycle of angular momentum.

$$\left(\frac{da}{dt}\right)_{\vec{E}} = 0 \tag{4.10}$$

where a is the length of the semi-major axis.

The progressive distortion of the orbits by the electric field means that the particles never follow truly elliptical orbits, however the separation of the two turning points on each circuit around the nucleus is conserved and for field strengths well below the ionisation field strength the path around each circuit is almost elliptical.

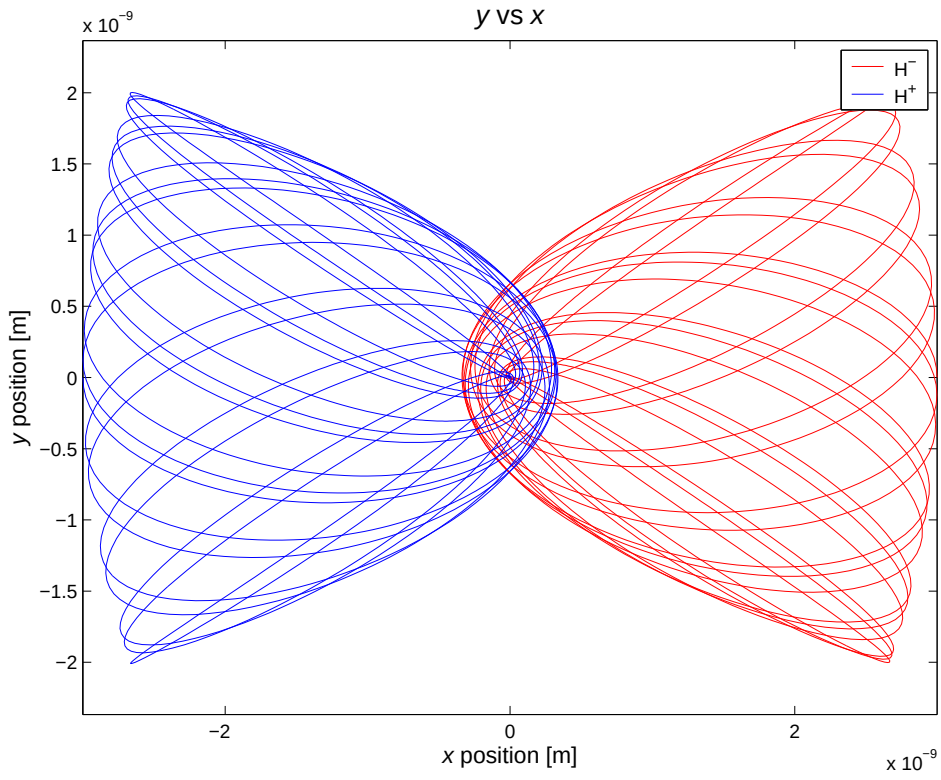

Figure 4.9: The H^+/H^- system, initial orbital eccentricity $\epsilon = 0.837$, subjected to a strong electric field $\vec{E} = 8 \times 10^5 V m^{-1} \hat{x}$.

Chapter 5

The quantum mechanical view of the Stark effect

The quantum mechanical view of the Stark effect relates to the reorganisation of atomic energy levels due to the application of an external field. In hydrogen-like atoms (such as Rydberg atoms) the different l states of a given n are degenerate; the application of an electric field lifts this degeneracy. The eigenfunctions of each Stark state are superpositions of the unperturbed eigenfunctions of different l states.

5.1 Calculating the Stark shifts

Starting with the non-relativistic Schrödinger equation we have

$$E\Psi = \left[-\frac{\hbar^2}{2m_e}\nabla^2 + V + \Phi\right]\Psi \tag{5.1}$$

where $\Phi = eE_x x$ is the perturbation potential (energy) due to the applied field, $V = -\frac{kZe^2}{r}$ is the Coulomb potential energy and ∇^2 is the Laplacian operator.

The expectation value of the perturbation potential is given by

$$\langle\Phi\rangle = \iint |\Psi_0^2|\,\Phi\,dxdy. \tag{5.2}$$

After a spatial inversion ($r \longrightarrow -r$), the field free, Coulombic Hamiltonian is unchanged; the field free eigenstates have a definite parity (*even* if unchanged by inversion, *odd* if sign changes), but $|\Psi_0^2|$ is unaffected. The perturbation Hamiltonian Φ however, has odd parity under spatial inversion and thus the expectation value $\langle\Phi\rangle$ vanishes.

The same argument holds for the matrix element between two unperturbed states Ψ_1 & Ψ_2, the corresponding matrix element of Φ will be zero unless the two states have opposite parity.

From the inversion of spherical harmonics we have

$$\Upsilon_{l,m}(\theta+\pi,\phi+\pi) = (-1)^l \Upsilon_{l,m}(\theta,\phi). \tag{5.3}$$

This tells us that an electron in a central potential, in a state l, m has even parity if l is even, odd parity if l is odd and hence Φ only has non-zero matrix elements for transitions with $\Delta l = \pm 1$.

First order perturbation theory gives Stark shifts with a linear dependence on field strength; these can be determined using the perturbation matrix $\mathbf{\Phi}$, with the spherical polar eigenfunctions used to calculate the eigenvalues of each element, however the Schrödinger equation remains seperable with an external field if expressed in *parabolic coordinates* [5].

5.1.1 Separating the Schrödinger equation

We must now re-express the various terms of the Schrödinger equation in terms of the parabolic coordinates ξ & η

where

$$x = \frac{1}{2}(\xi - \eta), \qquad\qquad y = \sqrt{\xi\eta}.$$

The perturbation potential energy is now given by

$$\Phi = \frac{1}{2} e E_x (\xi - \eta), \tag{5.4}$$

while the Coulomb potential energy becomes

$$V = -\frac{2kZe^2}{\xi + \eta}, \tag{5.5}$$

and the two-dimensional Laplacian operator, acting on our wavefunction is given by

$$\nabla^2\Psi = \frac{4}{\xi + \eta}\left[\frac{\partial}{\partial\xi}\left(\xi\frac{\partial\Psi}{\partial\xi}\right) + \frac{\partial}{\partial\eta}\left(\eta\frac{\partial\Psi}{\partial\eta}\right)\right].$$

Substituting in these terms gives

$$E\Psi = -\frac{\hbar^2}{2m_e}\left(\frac{4}{\xi + \eta}\right)\left[\frac{\partial}{\partial\xi}\left(\xi\frac{\partial\Psi}{\partial\xi}\right) + \frac{\partial}{\partial\eta}\left(\eta\frac{\partial\Psi}{\partial\eta}\right)\right] - \left(\frac{2kZe^2}{\xi + \eta} + \frac{1}{2}eE_x(\xi - \eta)\right)\Psi \tag{5.6}$$

multiplying by $\frac{1}{2}(\xi + \eta)$ and bringing all terms to one side we have

$$\frac{\hbar^2}{m_e}\left[\frac{\partial}{\partial\xi}\left(\xi\frac{\partial\Psi}{\partial\xi}\right) + \frac{\partial}{\partial\eta}\left(\eta\frac{\partial\Psi}{\partial\eta}\right)\right] + \left[\frac{1}{2}E(\xi + \eta) + kZe^2 + \frac{1}{4}eE_x(\xi^2 - \eta^2)\right]\Psi = 0 \tag{5.7}$$

To facilitate separation of the variables we assume Ψ is of the form

$$\Psi = \psi_1(\xi)\psi_2(\eta) \tag{5.8}$$

and equate the atomic number Z to the sum of the two separation perameters Z_1 & Z_2

$$Z = Z_1 + Z_2 \tag{5.9}$$

Substituting equation 5.8 into equation 5.7 allows separation into two differential equations (5.10 & 5.11), each depending on a single varible

$$\frac{\hbar^2}{m_e}\frac{\partial}{\partial\xi}\left(\xi\frac{\partial\psi_1}{\partial\xi}\right) + \left(\frac{1}{2}E\xi + kZ_1e^2 - \frac{1}{4}eE_x\xi^2\right)\psi_1 = 0 \tag{5.10}$$

$$\frac{\hbar^2}{m_e}\frac{\partial}{\partial\eta}\left(\eta\frac{\partial\psi_2}{\partial\eta}\right) + \left(\frac{1}{2}E\eta + kZ_2e^2 + \frac{1}{4}eE_x\eta^2\right)\psi_2 = 0 \tag{5.11}$$

In order to solve these equations we must eliminate the derivatives in equations 5.10 & 5.11, using the following substitutions

$$\Lambda_1 = \psi_1\sqrt{\xi}, \qquad \Lambda_2 = \psi_2\sqrt{\eta}.$$

After making these substitutions our two differential equations become

$$\frac{d^2\Lambda_1}{d\xi^2} + \Gamma_1\psi_1\sqrt{\xi} = 0, \tag{5.12}$$

$$\frac{d^2\Lambda_2}{d\eta^2} + \Gamma_2\psi_2\sqrt{\eta} = 0, \tag{5.13}$$

where

$$\Gamma_1 = \frac{E}{2} + \frac{kZ_1e^2}{\xi} - \frac{1}{4}eE_x\xi, \tag{5.14}$$

$$\Gamma_2 = \frac{E}{2} + \frac{kZ_2e^2}{\eta} + \frac{1}{4}eE_x\eta. \tag{5.15}$$

The derivation of the Stark shifted energy states in terms of the parabolic quantum numbers n_1 & n_2 comes from

$$\int\sqrt{\Gamma_1(x)}dx = \left(n_1 + \frac{1}{2}\right)\pi \tag{5.16}$$

and

$$\int\sqrt{\Gamma_2(x)}dx = \left(n_2 + \frac{1}{2}\right)\pi \tag{5.17}$$

where the electric field vector points in the positive x-direction.

5.1.2 Stark splitting

The expression for the second order Stark energy shift [1] comes from perturbation theory

$$W_{nn_1n_2m} = -\frac{Ry}{n^2} + \frac{3a_0eEn}{2}(n_1 - n_2) - \frac{a_0^2e^2E^2n^4}{32Ry}[17n^2 - 3(n_1 - n_2)^2 - 9m^2 + 19]. \tag{5.18}$$

Figure 5.1 is a plot of the Stark shifts as a function of electric field strength.

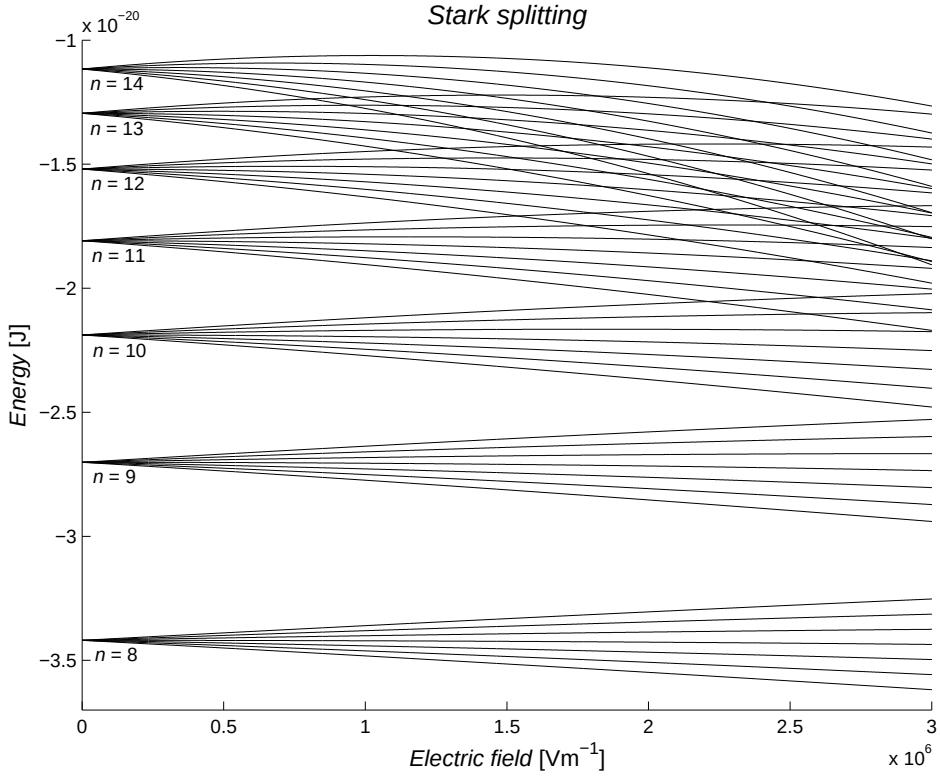

Figure 5.1: Second order Stark shifts in hydrogen for $|m| = 1$, $(n_1 - n_2) =$ n-4, n-2, ..., $-n+2, -n+4$; higher n states experience a greater energy shift for a given electric field strength.

5.2 Period of angular momentum oscillation

In chapter 4 we analysed the period of the long time-period oscillations in angular momentum, as a function of the electric field strength. We obtained a value using data from the simulation to determine a classical result

$$C = 6.95 \times 10^{-6} V s m^{-1}. \tag{5.19}$$

In order to test the accuracy of the simulation's results and provide a link to the quantum mechanical description of the Stark effect, we will now provide an analytical derivation of C in terms of fundamental constants.

5.2.1 Derivation of "C"

We start from the equation for the first order Stark energy shift [1]

$$\Delta W = \frac{3}{2} n e a_0 |\vec{E}| (n_1 - n_2) \tag{5.20}$$

where

$$\Delta W = \frac{h}{\tau}.$$

This allows us to derive an expression for the time-period τ as a function of electric field strength $E = |\vec{E}|$ and hence derive an expression for C dependent on the principle quantum number n

$$\tau = \frac{2h}{3nea_0 E} \tag{5.21}$$

$$\Rightarrow C = \frac{2h}{3nea_0} \tag{5.22}$$

5.2.2 Comparing the quantum and classical values for C

Substituting our value for C (see equation 5.19 above) obtained from the (entirely classical) simulation into the above quantum mechanical equation gives a value for the principle quantum number $n \approx 7.5$. Substituting this into equation 1.3 from chapter 1, which gives the radius of an atom with principle quantum number n, gives a radius of almost exactly 3nm; in perfect agreement with the simulation.

5.3 Ionising effects

From a quantum mechanical point of view, ionisation becomes a much more complicated problem than that described in section 4.1.2. Classically an atom with energy lower than the saddle point of the potential cannot escape, as it will not have enough kinetic energy to overcome the barrier bounding the local minima of potential close to the nucleus.

Providing the field strength is high enough, the anode creating the external field will be at a lower potential and there is a non-zero probability that the electron will tunnel through the barrier and be accelerated away from the atom towards the anode. The atom has been ionised.

A valence electron with energy above the saddle point is defined as unbound as it has sufficient kinetic energy to overcome the potential barrier and escape the atom. In reality the electron can only escape if its wavefunction is localised close to the saddle point, otherwise the electron remains dynamically bound even if it is energetically unbound. Of course there is no contradiction here, the confusion stems from two different definitions, one based on observation and the other on classical theory.

Chapter 6

A classical analytical approach

Until now all classical results presented have come from purely numerical simulations. Although the results seem fairly reliable, maintaing conservation laws and the correct relationships between physical quantities, it seems worthwhile to try and obtain an analytical solution to the equations of motion, both as a test of the numerical simulations and for the additional physical understanding such an exercise can bring.

6.1 Equations of motion

The MATLAB simulations are based on equations of motion for the coordinates and their time-derivatives, leading (in the two dimensional case) to four equations:

$$\frac{d\vec{x}}{dt} = \vec{v}_x, \qquad \frac{d\vec{y}}{dt} = \vec{v}_y \tag{6.1}$$

$$\frac{d\vec{v}_x}{dt} = \frac{\vec{F}_x}{m}, \qquad \frac{d\vec{v}_y}{dt} = \frac{\vec{F}_y}{m} \tag{6.2}$$

where $\vec{F}_x, \vec{F}_y$ come from Coulomb's law:

$$\vec{F}_x = -\frac{kZe^2}{\vec{r}}cos\theta + q\vec{E}_x, \qquad \vec{F}_y = -\frac{kZe^2}{\vec{r}}sin\theta + q\vec{E}_y \tag{6.3}$$

The inclusion of the force due to the externally applied electric field, unfortunately makes these particular equations insoluble by analytical methods, however a path to a solution was suggested in a 1964 paper on the properties of the Runge-Lenz vector [9]. This new approach was based on the use of *parabolic coordinates* in solving the Lagrange equation to find analytical solutions for the time-dependence of the coordinates. The Lagrange equation is based on the Lagrangian, which is defined as the difference between the kinetic and potential energies:

$$L = T - U \tag{6.4}$$

From the Lagrange equation:

$$\frac{\partial L}{\partial q_i} - \frac{d}{dt}\left(\frac{\partial L}{\partial \dot{q}_i}\right) = 0 \tag{6.5}$$

(where q_i is the i^{th} coordinate of our coordinate system) we obtained the following equations of motion for the parabolic coordinates ξ & η:

$$\frac{1}{8}m\left[\frac{\dot{\xi}^2\eta}{\xi^2} - \frac{2}{\xi}(\dot{\xi}\dot{\eta} + \ddot{\xi}\eta) + \frac{\dot{\eta}^2}{\eta} - 2\ddot{\xi}\right] - \frac{2kZe^2}{(\xi+\eta)^2} - \frac{eE_x}{2} - \frac{eE_y}{2}\sqrt{\frac{\eta}{\xi}} = 0 \tag{6.6}$$

$$\frac{1}{8}m\left[\frac{\dot{\eta}^2\xi}{\eta^2} - \frac{2}{\eta}(\dot{\eta}\dot{\xi} + \ddot{\eta}\xi) + \frac{\dot{\xi}^2}{\xi} - 2\ddot{\eta}\right] - \frac{2kZe^2}{(\eta+\xi)^2} + \frac{eE_x}{2} - \frac{eE_y}{2}\sqrt{\frac{\xi}{\eta}} = 0 \tag{6.7}$$

The full derivation of these equations of motion is given in appendix B.

The original problem, expressed in terms of Newtonian mechanics, has now been re-expressed in terms of Lagrangian mechanics; the two are exactly equivalent as they both express the state of a mechanical system in terms of its coordinates and their time-derivatives. Although this has resulted in a new set of equations, they do not seem immediately solvable, so it becomes necessary to make a transformation to a different set of independent variables.

6.2 Hamiltonian mechanics

A natural progression from the use of Lagrangian mechanics is Hamiltonian mechanics, which describes the state of a given system in terms of the coordinates and the corresponding components of the momentum. The Hamiltonian is better known as the quantum mechanical energy operator, but there is a corresponding classical Hamiltonian that is widely applicable in classical mechanics, given by:

$$H(q,p,t) = \sum_n p_n \dot{q}_n - L. \tag{6.8}$$

Also important in this formulation of mechanics is the *action*, defined as:

$$S = \int_{t_1}^{t_2} L dt, \tag{6.9}$$

and related to the Hamiltonian by the Hamilton-Jacobi equation:

$$\frac{\partial S}{\partial t} + H\left(q_i, p_i, t\right) = 0 \tag{6.10}$$

where

$$\frac{\partial S}{\partial q_i} = p_i \tag{6.11}$$

In order to solve the equations of motion, first you must find the *complete integral* of the Hamilton-Jacobi equation (i.e with as many independent arbitrary constants as there are independent variables). The independent variables in the model are simply the coordinates and time leading in the 2D case to 3 arbitrary constants.

6.3 Separation of variables

In chapter 5 parabolic coordinates were used to separate the Schrödinger equation. Having done this it was suggested that if the Schrödinger equation is separable, then the classical equations of motion for the same system should also be separable.

We have our Lagrangian in parabolic coordinates (derived in appendix B)

$$L = \frac{1}{8}m(\xi+\eta)\left(\frac{\dot{\xi}^2}{\xi}+\frac{\dot{\eta}^2}{\eta}\right) - U(\xi,\eta) \tag{6.12}$$

where the potential enegy U is given by

$$U = -\frac{2kZe^2}{\xi+\eta} + \frac{eE_x}{2}(\xi-\eta) + eE_y\sqrt{\xi\eta}. \tag{6.13}$$

The physically interesting cases of separable variables in parabolic coordinates, correspond to a potential energy of the form [7]

$$U = \frac{a(\xi)+b(\eta)}{\xi+\eta}. \tag{6.14}$$

If we choose $E_y = 0$[1] then our potential energy is of the correct form, where

$$a(\xi) = eE_x\xi^2 - kZe^2, \tag{6.15}$$

and

$$b(\eta) = -eE_x\eta^2 - kZe^2. \tag{6.16}$$

Our system is conservative so the Hamiltonian is simply the total energy and does not depend explicitly on time and the time dependence of the action is simplified. We wish to find a solution of the form

$$S = S_1(\xi) + S_2(\eta) - Et. \tag{6.17}$$

The Hamiltonian is given by

$$H = T + U \tag{6.18}$$

$$\Rightarrow H = \frac{2}{m(\xi+\eta)}\left[\xi\left(\frac{\partial S}{\partial \xi}\right)^2 + \eta\left(\frac{\partial S}{\partial \eta}\right)^2\right] + U(\xi,\eta) \tag{6.19}$$

[1]Any 2D coordinate system can be rotated such that $E_y = 0$

where $\frac{\partial S}{\partial q_i} = p_i$.

Substituting in equation 6.17, leads to two equations, each dependent on a single variable

$$2\xi \left(\frac{dS_1}{d\xi}\right)^2 + m(eE_x\xi^2 - kZe^2) - mE\xi = \Theta \tag{6.20}$$

$$2\eta \left(\frac{dS_2}{d\eta}\right)^2 - m(eE_x\eta^2 + kZe^2) - mE\eta = -\Theta \tag{6.21}$$

where Θ is a constant.

If these equations are rearranged in terms of S_1 & S_2, integration and summation together with the time-dependent term $-Et$ leads to the solution

$$S = -Et + \int \sqrt{\left[\frac{1}{2}mE + \frac{\Theta}{2\xi} - \frac{m(eE_x\xi^2 - kZe^2)}{2\xi}\right]} d\xi + \int \sqrt{\left[\frac{1}{2}mE - \frac{\Theta}{2\eta} + \frac{m(eE_x\xi^2 + kZe^2)}{2\eta}\right]} d\eta. \tag{6.22}$$

Unfortunately these equations remain unsolvable except through numerical techniques. Much is made in the literature of how useful the transition to parabolic coordinates is for the Stark-Coulomb problem [1] [5] [7], however the final solution does not appear to have been reached. Separable does not imply solvable.

Chapter 7

The Runge-Lenz vector

For a trajectory in a hydrogenic potential there are two vector constants of motion; the angular momentum $\vec{L}$ (discussed in chapter 4) and the dimensionless Runge-Lenz vector $\vec{A}$, given by equation 7.1

$$\vec{A} = \hat{r} + \frac{(\vec{L} \times \vec{p})}{kZe^2m}. \tag{7.1}$$

The Runge-Lenz vector was first described by Lenz in 1924 [8], and was used by Pauli only two years later to analytically determine the energy levels of hydrogen.

7.1 The Runge-Lenz vector in an electric field

With the application of an external electric field, the electron in a Rydberg atom feels a continuously changing torque with the result that neither the angular momentum nor the Runge-Lenz vector are conserved.

The idea to use the Runge-Lenz vector as a basis for studying hydrogenic atoms in external electric fields, came from a 1963 paper [9] in which a generalisation $\vec{C}$ of the Runge-Lenz vector is obtained that remains conserved in the combined Coulomb/Stark potential.

7.2 Deriving the generalised Runge-Lenz vector

Equation 7.2 is the equation of motion for a particle in Coulomb-Stark potential

$$\frac{d\vec{p}}{dt} = -\frac{kZe^2}{r^2}\hat{r} + e\vec{E} \tag{7.2}$$

The rate of change of angular momentum, due to the torque applied by the external field is given by

$$\frac{d\vec{L}}{dt} = e(\vec{r} \times \vec{E}). \tag{7.3}$$

The key to the rest of the derivation is the observation that

$$\frac{d\hat{r}}{dt} = \frac{1}{mr^2}(\vec{L} \times \hat{r}) \tag{7.4}$$

see equations 7.5 & 7.6

$$d\hat{r} = d\theta\hat{\theta} \;\; \Rightarrow \;\; \frac{d\hat{r}}{dt} = \frac{d\theta}{dt}\hat{\theta} = \omega\hat{\theta} \;\; \Rightarrow \;\; \left|\frac{d\hat{r}}{dt}\right| = \omega \tag{7.5}$$

$$\left|\frac{1}{mr^2}(\vec{L} \times \hat{r})\right| = \frac{|\vec{r}| \times |\vec{p}|}{mr^2} = \frac{mr^2\omega}{mr^2} = \omega. \tag{7.6}$$

In order to derive a vector that remains constant in an external field, we need to know how the rate of change of $\vec{A}$ (see equation 7.1) depends on the electric field

$$\frac{d}{dt}(\vec{L} \times \vec{p}) = \left(\frac{d\vec{L}}{dt} \times \vec{p}\right) + \left(\vec{L} \times \frac{d\vec{p}}{dt}\right).$$

Substituting in the equations of motion (equations 7.2 & 7.3) we have

$$\frac{d}{dt}(\vec{L} \times \vec{p}) = e(\vec{r} \times \vec{E}) \times \vec{p} + \vec{L} \times \left(-\frac{kZe^2}{r^2}\hat{r} + e\vec{E}\right) \tag{7.7}$$

$$= e(\vec{L} \times \vec{E}) - \frac{kZe^2}{r^2}(\vec{L} \times \hat{r}) + e(\vec{r} \times \vec{E}) \times \vec{p}. \tag{7.8}$$

Now we can calculate the rate of change of $\vec{A}$

$$\frac{d\vec{A}}{dt} = \frac{d\hat{r}}{dt} + \frac{1}{kZe^2m}\frac{d}{dt}(\vec{L} \times \vec{p}) \tag{7.9}$$

substituting in from equations 7.4 & 7.8 we have

$$\frac{d\vec{A}}{dt} = \frac{1}{mr^2}(\vec{L} \times \hat{r}) + \frac{1}{kZe^2m}\left[e(\vec{L} \times \vec{E}) - \frac{kZe^2}{r^2}(\vec{L} \times \hat{r}) + e(\vec{r} \times \vec{E}) \times \vec{p}\right] \tag{7.10}$$

which reduces to

$$\frac{d\vec{A}}{dt} = \frac{1}{kZe^2m}\left[e(\vec{L} \times \vec{E}) + e(\vec{r} \times \vec{E}) \times \vec{p}\right]. \tag{7.11}$$

We get another relationship between $\vec{A}$ & $\vec{E}$ from

$$\frac{d}{dt}(\vec{A}.\vec{E}) = \frac{d\vec{A}}{dt}.\vec{E} + \frac{d\vec{E}}{dt}.\vec{A} \tag{7.12}$$

but the electric field is assumed to be constant so we can ignore the rate of change of $\vec{E}$ and substitute equation 7.11 into the remaining term

$$\frac{d}{dt}(\vec{A}.\vec{E}) = \frac{1}{kZem}(\vec{r} \times \vec{E}).(\vec{p} \times \vec{E})$$

$$= \frac{1}{2kZe}\frac{d}{dt}(\vec{r} \times \vec{E})^2. \tag{7.13}$$

Bringing all terms to one side of the equation we have

$$\frac{d}{dt}\left(\vec{A}.\vec{E} - \frac{1}{2kZe}(\vec{r} \times \vec{E})^2\right) = 0 \tag{7.14}$$

$$= \frac{d}{dt}(\vec{C}.\vec{E}).$$

The generalised Runge-Lenz vector $\vec{C}$ is given by equation 7.15

$$\vec{C} = \vec{A} - \frac{[(\vec{r} \times \vec{E}) \times \vec{r}]}{2kZe}. \tag{7.15}$$

7.3 The Runge-Lenz vector in the simulation

The vector $\vec{A}$ is always directed along the major-axis of the ellipse; if the orbit is circular, then $\vec{A} = 0$. Reducing the initial velocity of the electron in the simulation gives an elliptical orbit, with the major-axis oriented along the x-axis; figure 7.1 plots the conserved component of the Runge-Lenz vector A_x, against time.

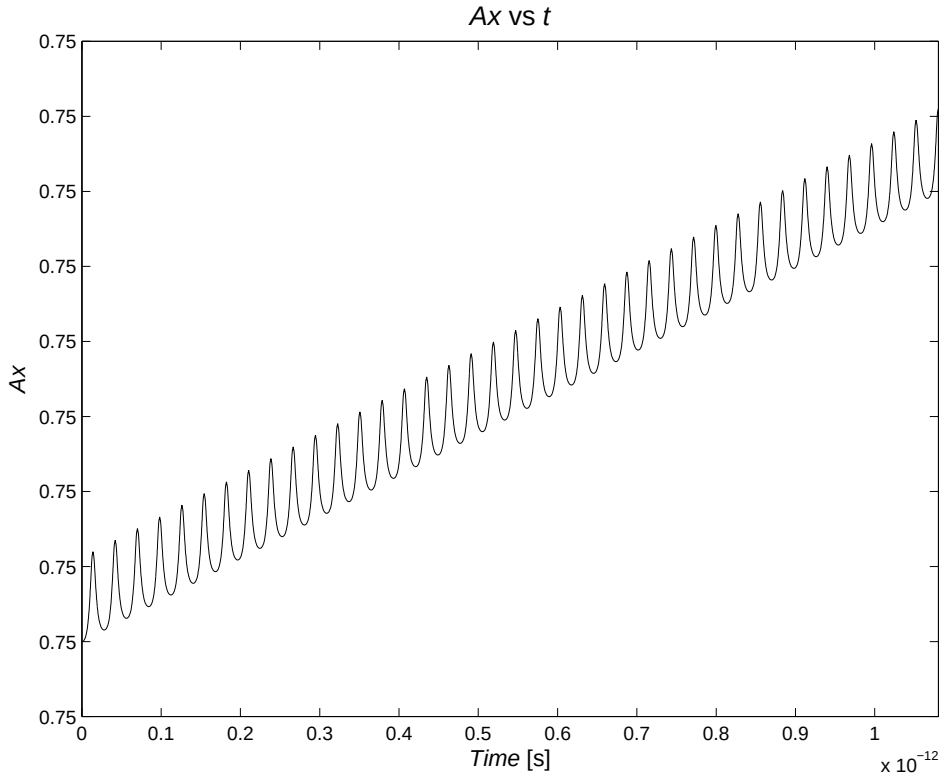

Figure 7.1: $\vec{A}$ is conserved in the abscence of an electric field.

Numerical errors mean the the simulation produces small changes in the component of $\vec{A}$ & $\vec{C}$.

With the application of a constant electric field in the x-direction, $\vec{A}$ is no longer conserved and we must revert to $\vec{C}$. $\vec{C}$ also points along the major-axis, so in the case of a circular orbit $\vec{C} = \vec{A} = 0$ and in the case where $\vec{E} = 0$, $\vec{C} = \vec{A}$.

To test our derivation of $\vec{C}$, figure 7.2 plots C_x against time for an electric field: $\vec{E} = 3 \times 10^6 V m^{-1} \hat{x}$

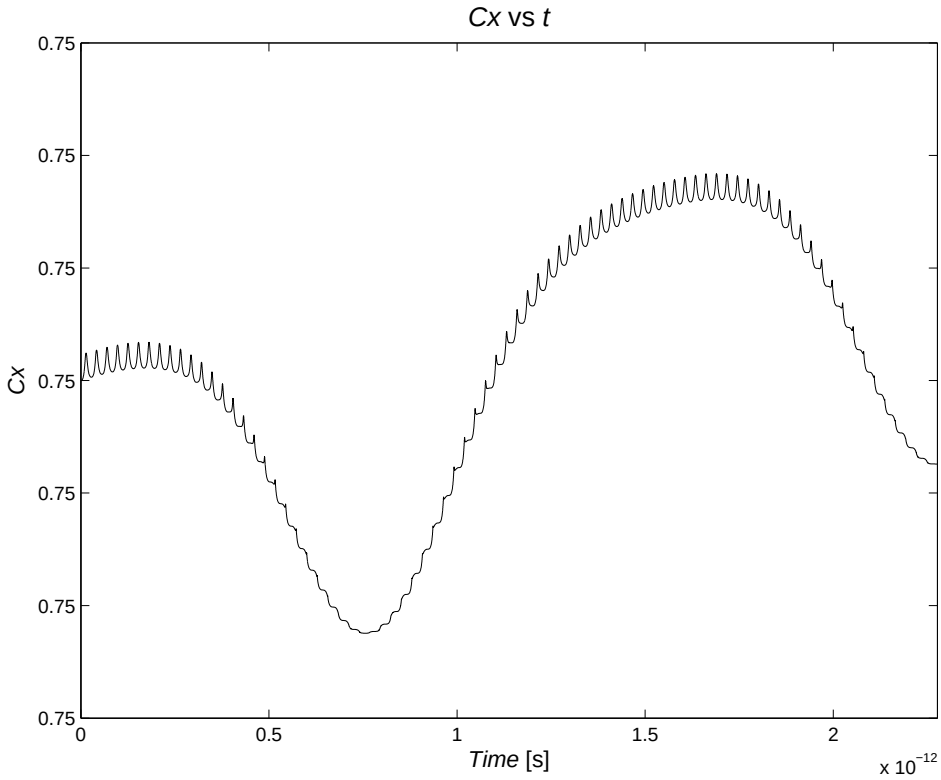

Figure 7.2: The component of $\vec{C}$ along the major-axis is conserved, even in the presence of an electric field.

7.4 Calculations with the Runge-Lenz vector

Going through the derivation for the generalised Runge-Lenz vector gives a great deal of insight into the geometry of the Coulomb-Stark problem. There are various calculations that can be done using $\vec{A}$, regarding the envelope of the orbit

$$|\vec{A}| = \epsilon \equiv eccentricity$$

$$\Rightarrow |\vec{A}| = \sqrt{1 - \left(\frac{b}{a}\right)^2} \tag{7.16}$$

where: $a \equiv$ semi-major axis & $b \equiv$ semi-minor axis.

Figure 7.3 gives a graphical representation of $\vec{A}$ for an elliptical orbit with no external field

As a further test of the accuracy of the simulation we plug the conserved value

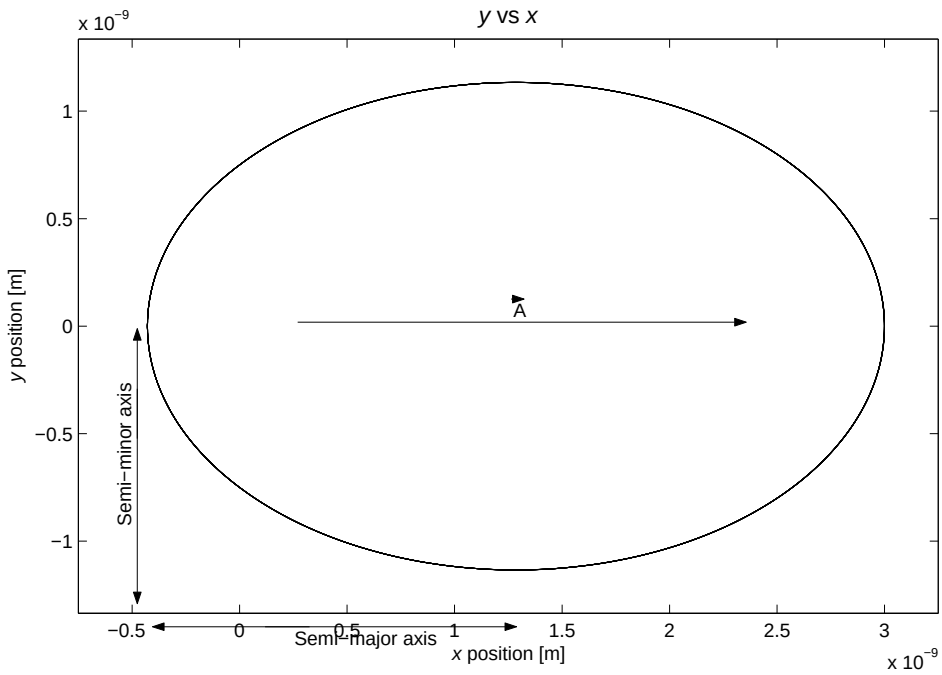

Figure 7.3: The component of $\vec{A}$ along the major-axis is conserved in the abscence of an electric field.

of $|\vec{A}|$ into equation 7.16

$$a = 1.714 \times 10^{-9} m$$

$$b = 1.134 \times 10^{-9} m$$

$$\Rightarrow \epsilon = 0.7499$$

where: $|\vec{A}| = 0.75$.

Chapter 8

Three dimensional simulations

It was fairly early on in the project that I first extended the hydrogen atom in a Stark field simulation into three dimensions; up until then all motion had been confined to the $x-y$ plane. The initial conditions are identical to the two dimensional version (i.e. $z(0) = 0, v_z(0) = 0$), however we now add an external field with components oriented along the y & z axes.

8.1 Angular momentum in 3D

The two dimensional simulations above have $|L| = L_z$, movement out of the plane results in non-zero angular momentum components about all three axes. Although the three dimensional plots can often just look like big balls of string, examination of the trajectory looking along the three axes, compared with plots of the angular momentum about the respective axes can give a good idea of the behaviour of the particle. The $x-y$ motion and the resulting $L_z(t)$ are shown in figure 8.1.

The $x-y$ plot shows a similar outline to the original two dimensional plots (rotated through 90^o because there is now an electric field component along the y-axis but not the x-axis) with further complications due to motion out of the plane. The z-component of the angular momentum still has the same form (see section 4.1.1), but now it stays positive at all times, meaning the the direction of

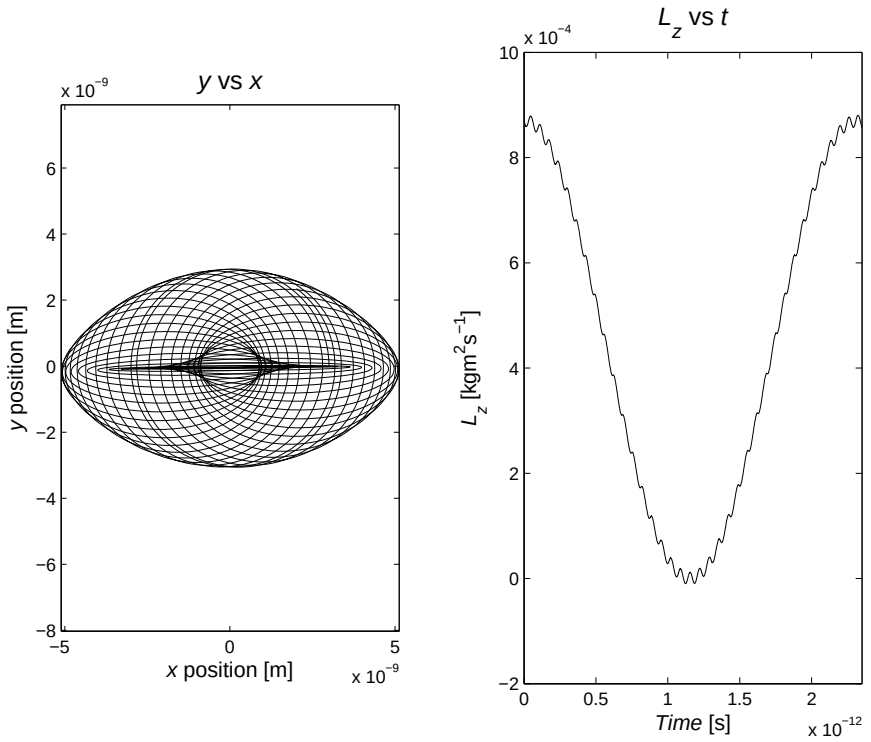

Figure 8.1: Initially on a circular orbit, of radius $3nm$ in the $x-y$ plane, $E_y = E_z = 2.16 \times 10^6 Vm^{-1}$.

rotation in the $x-y$ plane never changes sense.

Angular momentum about the y-axis is initially zero, however the momentum from the initial velocity in the positive y direction, combined with the force applied by the field component pointing along z axis, causes the electron to aquire an angular momentum component L_y. Figure 8.2 shows the $z-x$ trajectory and the associated angular momentum component $L_y(t)$; notice that the equal electric field components along the y & z axes cause an apparent oscillation of angular momentum between L_y & L_z,

$$\begin{aligned} L_y = 0 \quad &\Rightarrow \quad L_z = L_z^{[max]}, \\ L_z = 0 \quad &\Rightarrow \quad L_y = L_y^{[max]}. \end{aligned}$$

Viewing the trajectory in the $y-z$ plane (i.e. along the axis with no electric field component) ties the picture together; see figure 8.3. The ends of the loops form flat, diagonal lines, parallel to the line $y = z$, because components of motion perpendicular to the electric field, are unaffected.

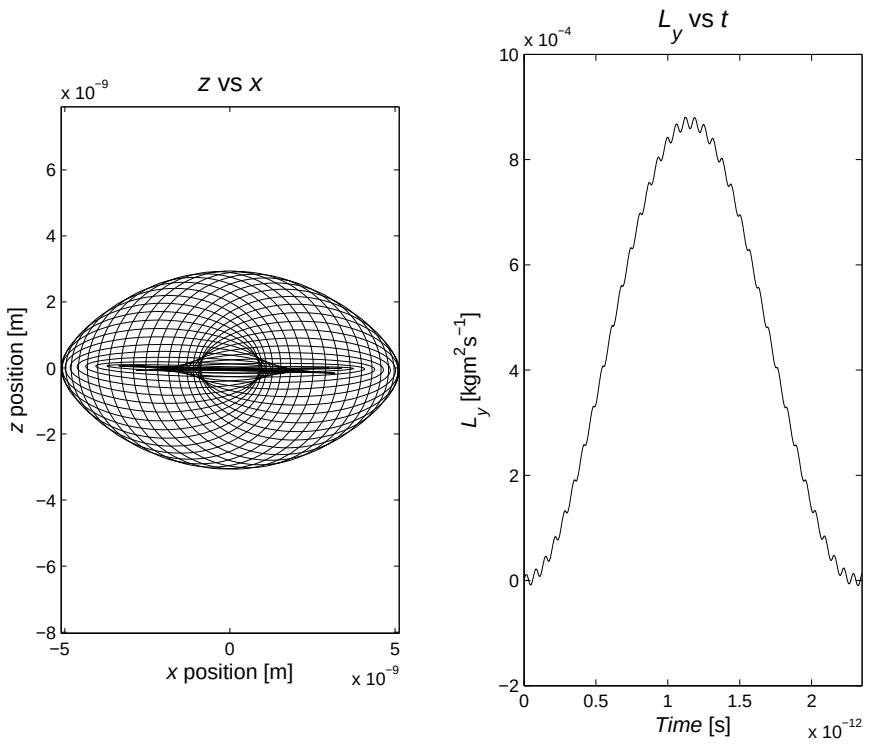

Figure 8.2: The angular momentum component L_y shows similar behaviour to L_z, but inverted.

This is analogous to the conservation of the generalised Runge-Lenz vector (see equation 7.15), here the component of $\vec{r}$ perpendicular to $\vec{E}$ is conserved.

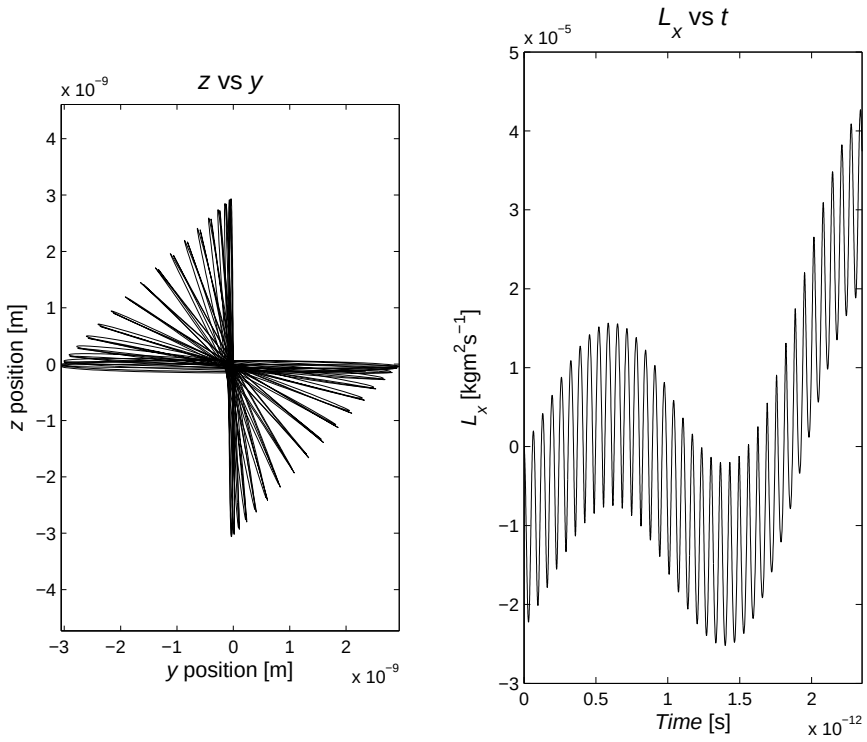

Figure 8.3: The oscillation of L_x (positive and negative) is what causes the transfer of angular momentum between L_y & L_z.

Chapter 9

Conclusion

Rydberg systems have proved extremely important in the development of modern atomic physics. While many of their properties have been successfully predicted by extrapolation from low lying states, the most interesting areas for study centre around those effects specific to Rydberg systems, notably the response to electric and magnetic fields (the Stark and Zeeman effects respectively). Ground state atoms are practically unaffected except by extraordinarily high field strengths.

This high susceptability to perturbation by even very weak radiation fields has led to many fascinating experiments, impossible in less excited atoms. A particular example is the single atom *micromaser*; the long wavelenths characteristic of the radiation from between Rydberg states simplifies the contruction of the resonant cavity. While investigations of the response of atoms to high strength radiation fields has also centred around Rydberg atoms, their exaggerated response makes it possible to make quantitative measurements to a very high degree of precision.

The work in this project has concentrated on the Stark effect in Rydberg systems, as this has often been neglected in favour of the Zeeman effect [11]. The simulations presented in this project have demonstrated the close similarities between conventional and heavy Rydberg atoms and the advantages to be gained from conducting novel experiments on the latter [13].

We have also seen that many of the properties of Rydberg systems can be reproduced in an entirely classical simulation. Comparisons of the simulated classical Stark effect with the results of quantum mechanical calculations demonstrate

the correspondence principle linking classical and quantum mechanics.

Appendix A

The Runge-Kutta algorithm

This excellent technique for the numerical solution of systems of differential equations was developed in 1901 by Carle Runge and Martin Kutta in order to address the shortcomings of the ubiquitous Euler technique.

A.1 First order

Suppose there are two variables: x and y and two differential equations:

$$x' = f(t, x, y) \qquad y' = g(t, x, y)$$

x_n is the value of x at time t_n, and similarly for y_n.

The first order algorithm is based on a Taylor series expansion of each of the two functions about the midpoint of the integration interval h:

$$f(t, x, y) \approx f(t_{n+1/2}, x_{n+1/2}, y_{n+1/2}) + (t - t_{n+1/2})\frac{df}{dt}$$
$$g(t, x, y) \approx g(t_{n+1/2}, x_{n+1/2}, y_{n+1/2}) + (t - t_{n+1/2})\frac{df}{dt}$$

The technique uses the derivative of the function, evaluated at the midpoint of the integration interval to produce an approximate solution for the end of the interval. This gives an error proportional to h^3, an order of magnitude better than the Euler technique.

A.2 Fourth order

The algorithm used in the simulation is in fact the fourth order Runge-Kutta, in which four sample points are used within each interval and a weighted average used to calculate the approximate solution for the end of the interval. This gives a numerical integration error proportional to h^5.

The formulae for the fourth order Runge-Kutta algorithm are:

$$x_{n+1} = x_n + (h/6)(p_1 + 2p_2 + 2p_3 + p_4)$$
$$y_{n+1} = y_n + (h/6)(q_1 + 2q_2 + 2q_3 + q_4)$$

where:

$$p_1 = f(t_n, x_n, y_n)$$
$$q_1 = g(t_n, x_n, y_n)$$
$$p_2 = f(t_n + h/2, x_n + (h/2)p_1, y_n + (h/2)q_1)$$
$$q_2 = g(t_n + h/2, x_n + (h/2)p_1, y_n + (h/2)q_1)$$
$$p_3 = f(t_n + h/2, x_n + (h/2)p_2, y_n + (h/2)q_2)$$
$$q_3 = g(t_n + h/2, x_n + (h/2)p_2, y_n + (h/2)q_2)$$
$$p_4 = f(t_n + h, x_n + hp_3, y_n + hq_3)$$
$$q_4 = g(t_n + h, x_n + hp_3, y_n + hq_3)$$

Given starting values x_0 & y_0 we can plug them into the formula to find x_1 & y_1. Then we can plug in x_1 & y_1 to find x_2 & y_2 and so on. [12] [14]

Appendix B

Derivation of the Lagrangian equations of motion in parabolic coordinates

Starting from the potential energy in equation B.1:

$$U = -\frac{kZe^2}{\sqrt{x^2+y^2}} + eE_x x + eE_y y \tag{B.1}$$

First we transform from x & y into the parabolic coordinates ξ & η:

$$x = \tfrac{1}{2}(\xi - \eta), \qquad\qquad y = \sqrt{\xi\eta}$$

The potential energy is now given by equation B.2

$$\Rightarrow U = -\frac{2kZe^2}{\xi+\eta} + \frac{eE_x}{2}(\xi-\eta) + eE_y\sqrt{\xi\eta} \tag{B.2}$$

In cartesian coordinates the kinetic energy is given by equation B.3:

$$T = \frac{1}{2}m\dot{x}^2 + \frac{1}{2}m\dot{y}^2 \tag{B.3}$$

The velocities in parabolic coordinates are given by:

$$\dot{x} = \tfrac{1}{2}(\dot{\xi} - \dot{\eta}), \qquad \dot{y} = \tfrac{1}{2}\left(\sqrt{\frac{\xi}{\eta}}\,\dot{\eta} + \sqrt{\frac{\eta}{\xi}}\,\dot{\xi}\right)$$

which gives the kinetic energy shown in equation B.4

$$\Rightarrow T = \frac{1}{8}m(\xi+\eta)\left(\frac{\dot{\xi}^2}{\xi}+\frac{\dot{\eta}^2}{\eta}\right) \tag{B.4}$$

The Lagrangian of a system is the difference between the kinetic and potential energies:

$$L = T - U$$

Equation B.5 is the Lagrangian for the system

$$\Rightarrow L = \frac{1}{8}m(\xi+\eta)\left(\frac{\dot{\xi}^2}{\xi}+\frac{\dot{\eta}^2}{\eta}\right)+\frac{2kZe^2}{\xi+\eta}-\frac{eE_x}{2}(\xi-\eta)-eE_y\sqrt{\xi\eta} \tag{B.5}$$

We now substitute into the Lagrange equation:

$$\frac{\partial L}{\partial q_i}-\frac{d}{dt}\left(\frac{\partial L}{\partial \dot{q}_i}\right)=0$$

where q_i is any generalised system of coordinates.

The parabolic, Lagrangian equations of motion are given in equations B.6 & B.7:

$$\frac{1}{8}m\left[\frac{\dot{\xi}^2\eta}{\xi^2}-\frac{2}{\xi}(\dot{\xi}\dot{\eta}+\ddot{\xi}\eta)+\frac{\dot{\eta}^2}{\eta}-2\ddot{\xi}\right]-\frac{2kZe^2}{(\xi+\eta)^2}-\frac{eE_x}{2}-\frac{eE_y}{2}\sqrt{\frac{\eta}{\xi}}=0 \tag{B.6}$$

$$\frac{1}{8}m\left[\frac{\dot{\eta}^2\xi}{\eta^2}-\frac{2}{\eta}(\dot{\eta}\dot{\xi}+\ddot{\eta}\xi)+\frac{\dot{\xi}^2}{\xi}-2\ddot{\eta}\right]-\frac{2kZe^2}{(\eta+\xi)^2}+\frac{eE_x}{2}-\frac{eE_y}{2}\sqrt{\frac{\xi}{\eta}}=0 \tag{B.7}$$

Appendix C

MATLAB simulation code

C.1 The 2D hydrogen atom simulation

```
clc; clear; clf;
m=9.11e-31;   Z=1;  k=8.99e9;  e=1.6e-19;   %Physical constants

notimesteps = 350000;          %Timesteps
v = zeros(notimesteps,26);

maxXX = 0; minXX = 0;          %Testing for max/min x,y limits
maxXY = 0; minXY = 0;
maxYY = 0; minYY = 0;
maxYX = 0; minYX = 0;

%Ex = 0; Ey = 0;               %Electric field
Ex = 3e6; Ey = 0;
%Ex = 0; Ey = 3e6;
%Ex = 2.12e6; Ey = 2.12e6;

Efield = sqrt(Ex^2 + Ey^2);

%Initial conditions

t0 = 0;
h0 = 5e-16;                    %Initial stepsize
x0 = 3e-9;
vx0= 0;
y0 = 0;
vy0= 290188.37643213599829660469770936; %Circular motion
u0 = sqrt(vx0^2 + vy0^2);
Fx0= -k*Z*e^2/(x0^2 + y0^2)*x0/sqrt(x0^2 + y0^2) - e*Ex;
Fy0= -k*Z*e^2/(x0^2 + y0^2)*y0/sqrt(x0^2 + y0^2) - e*Ey;
F0 = sqrt(Fx0^2 + Fy0^2);
th0= atan(y0/x0);
```

```
r0 = sqrt(x0^2 + y0^2);
T0 = m/2*(vx0^2 + vy0^2);
U0 = -k*Z*e^2/sqrt(x0^2 + y0^2) + e*(Ex*x0 + Ey*y0);
E0 = T0 + U0;
dE0= 0;
L0 = m*(x0*vy0 - y0*vx0); % = Lz0
px0= m*vx0;
py0= m*vy0;
p0 = sqrt(px0^2 + vy0^2);
Ax0= x0/r0 - L0*py0/(k*Z*e^2*m); %L _|_ P => sin@ = 1
Ay0= y0/r0 + L0*px0/(k*Z*e^2*m);
A0 = sqrt(Ax0^2 + Ay0^2);
Cx0= Ax0 - (Ex*y0^2 - Ey*x0*y0)/(2*k*Z*e);
Cy0= Ay0 - (Ey*x0^2 - Ex*x0*y0)/(2*k*Z*e);
C0 = sqrt(Cx0^2 + Cy0^2);

tmax = 23.5e-12;      %End simulation

v(1,1) = t0;      %1st row matrix elements
v(1,2) = h0;
v(1,3) = x0;
v(1,4) = vx0;
v(1,5) = y0;
v(1,6) = vy0;
v(1,7) = u0;
v(1,8) = Fx0;
v(1,9) = Fy0;
v(1,10)= F0;
v(1,11)= th0;
v(1,12)= r0;
v(1,13)= T0;
v(1,14)= U0;
v(1,15)= E0;
v(1,16)= dE0;
v(1,17)= L0;
v(1,18)= px0;
v(1,19)= py0;
v(1,20)= p0;
v(1,21)= Ax0;
v(1,22)= Ay0;
v(1,23)= A0;
v(1,24)= Cx0;
v(1,25)= Cy0;
v(1,26)= C0;

for n = (2:notimesteps)

    if v(n-1,12) > 10*r0   %If r > 10r0, end for loop
       disp('r > 10*r0'); break
    end

    if v(n-1,1)  > tmax   %If t > tmax, end for loop
       disp('t > tmax'); break
    end
```

```
%Time (t)
v(n,1) = v(n-1,1) + (v(n-1,12)/r0)^2*h0;    %Adaptive stepsize

%Stepsize (h)
v(n,2)= v(n,1) - v(n-1,1);

p1 = v(n-1,4);          %dx/dt = vx
q1 = -(k*Z*e^2)/m*v(n-1,3)/(v(n-1,3)^2 + v(n-1,5)^2)^(3/2) - e*Ex/m; %dvx/dt
r1 = v(n-1,6);          %dy/dt = vy
s1 = -(k*Z*e^2)/m*v(n-1,5)/(v(n-1,3)^2 + v(n-1,5)^2)^(3/2) - e*Ey/m; %dvy/dt

p2 = v(n-1,4) + v(n,2)/2*q1;
q2 = -(k*Z*e^2)/m*(v(n-1,3) + (v(n,2)/2*p1))/((v(n-1,3) + v(n,2)/2*p1)^2 + ...
                                    (v(n-1,5) + v(n,2)/2*r1)^2)^(3/2) - e*Ex/m;
r2 = v(n-1,6) + v(n,2)/2*s1;
s2 = -(k*Z*e^2)/m*(v(n-1,5) + (v(n,2)/2*r1))/((v(n-1,3) + v(n,2)/2*p1)^2 + ...
                                    (v(n-1,5) + v(n,2)/2*r1)^2)^(3/2) - e*Ey/m;

p3 = v(n-1,4) + v(n,2)/2*q2;
q3 = -(k*Z*e^2)/m*(v(n-1,3) + (v(n,2)/2*p2))/((v(n-1,3) + v(n,2)/2*p2)^2 + ...
                                    (v(n-1,5) + v(n,2)/2*r2)^2)^(3/2) - e*Ex/m;
r3 = v(n-1,6) + v(n,2)/2*s2;
s3 = -(k*Z*e^2)/m*(v(n-1,5) + (v(n,2)/2*r2))/((v(n-1,3) + v(n,2)/2*p2)^2 + ...
                                    (v(n-1,5) + v(n,2)/2*r2)^2)^(3/2) - e*Ey/m;

p4 = v(n-1,4) + v(n,2)*q3;
q4 = -(k*Z*e^2)/m*(v(n-1,3) + (v(n,2)*p3))/((v(n-1,3) + ...
   v(n,2)*p3)^2 + (v(n-1,5) + v(n,2)*r3)^2)^(3/2) - e*Ex/m;
r4 = v(n-1,6) + v(n,2)*s3;
s4 = -(k*Z*e^2)/m*(v(n-1,5) + (v(n,2)*r3))/((v(n-1,3) + ...
   v(n,2)*p3)^2 + (v(n-1,5) + v(n,2)*r3)^2)^(3/2) - e*Ey/m;

%x
v(n,3) = v(n-1,3) + (v(n,2)/6)*(p1 + 2*p2 + 2*p3 + p4);

%vx
v(n,4) = v(n-1,4) + (v(n,2)/6)*(q1 + 2*q2 + 2*q3 + q4);

%y
v(n,5) = v(n-1,5) + (v(n,2)/6)*(r1 + 2*r2 + 2*r3 + r4);

%vy
v(n,6) = v(n-1,6) + (v(n,2)/6)*(s1 + 2*s2 + 2*s3 + s4);

%v = u
v(n,7) = sqrt(v(n,4)^2 + v(n,6)^2);

%Fx
v(n,8) = -k*Z*e^2/(v(n,3)^2 + v(n,5)^2)*v(n,3)/sqrt(v(n,3)^2 + v(n,5)^2) - e*Ex;

%Fy
v(n,9) = -k*Z*e^2/(v(n,3)^2 + v(n,5)^2)*v(n,5)/sqrt(v(n,3)^2 + v(n,5)^2) - e*Ey;
```

```
%F
v(n,10) = sqrt(v(n,8)^2 + v(n,9)^2);

%theta
v(n,11) = atan(v(n,5)/v(n,3));

%r
v(n,12) = sqrt(v(n,3)^2 + v(n,5)^2);

%T(KE)
v(n,13)= (m/2)*(v(n,4)^2 + v(n,6)^2);

%U(PE)
v(n,14)= -k*Z*e^2/v(n,12) + e*(Ex*v(n,3) + Ey*v(n,5));

%E
v(n,15)= v(n,13) + v(n,14);

%deltaE
v(n,16)= v(n,15) - v(n-1,15);

%L = Lz
v(n,17)= m*(v(n,3)*v(n,6) - v(n,5)*v(n,4));

%px
v(n,18)= m*v(n,4);

%py
v(n,19)= m*v(n,6);

%p
v(n,20)= sqrt(v(n,18)^2 + v(n,19)^2);

%Ax
v(n,21)= v(n,3)/v(n,12) - v(n,17)*v(n,19)/(k*Z*e^2*m); %L at right angle to P

%Ay
v(n,22)= v(n,5)/v(n,12) + v(n,17)*v(n,18)/(k*Z*e^2*m);

%A
v(n,23)= sqrt(v(n,21)^2 + v(n,22)^2);

%Cx
v(n,24)= v(n,21) + (Ex*v(n,5)^2 - Ey*v(n,3)*v(n,5))/(2*k*Z*e);

%Cy
v(n,25)= v(n,22) + (Ey*v(n,3)^2 - Ex*v(n,3)*v(n,5))/(2*k*Z*e);

%C
v(n,26)= sqrt(v(n,24)^2 + v(n,25)^2);

if (v(n,3) >= maxXX)   %Testing for max/min x,y limits
   maxXX = v(n,3);
   maxXY = v(n,5);
```

```
    end
    if (v(n,3) <= minXX)
       minXX = v(n,3);
       minXY = v(n,5);
    end
    if (v(n,5) >= maxYY)
       maxYX = v(n,3);
       maxYY = v(n,5);
    end
    if (v(n,5) <= minYY)
       minYX = v(n,3);
       minYY = v(n,5);
    end
end

format short g;   %Chooses most appropriate format with 5 digits

w = v(1:n-1,:);

disp('       t            h            r            L           E');   %Display output
W = [w(:,1)];
disp(W);

t = w(:,1);
h = w(:,2);
x = w(:,3);
vx= w(:,4);
y = w(:,5);
vy= w(:,6);
u = w(:,7);
Fx= w(:,8);
Fy= w(:,9);
F = w(:,10);
th= w(:,11);
r = w(:,12);
T = w(:,13);
U = w(:,14);
E = w(:,15);
dE= w(:,16);
L = w(:,17);
px= w(:,18);
py= w(:,19);
p = w(:,20);
Ax= w(:,21);
Ay= w(:,22);
A = w(:,23);
Cx= w(:,24);
Cy= w(:,25);
C = w(:,26);

disp(n)       %Display no. of final timestep reached
disp(max(t))  %Display final time

apo = max(r);             %Apogee
```

```
peri= min(r);              %Perigee
majoraxis = apo + peri;    %Major-axis

P = [apo,peri,apo_peri];
disp('    apogee       perigee    apo + peri  initmajoraxis tiltmajoraxis')
disp(P)


%Display limits x/y limits

disp('max x')
disp('[x,y] =');
disp([maxXX,maxXY]);

disp('min x')
disp('[x,y] =');
disp([minXX,minXY]);

disp('max y')
disp('[x,y] =');
disp([maxYX,maxYY]);

disp('min y')
disp('[x,y] =');
disp([minYX,minYY]);


%Plotting figures

figure(1)
plot(x,y,'k-');
xlabel('{\itx} position [m]','fontsize',12);
ylabel('{\ity} position [m]','fontsize',12);
title('{\ity} vs {\itx}','fontsize',14);
axis([1.1*minXX 1.1*maxXX 1.1*minYY 1.1*maxYY]);
axis equal

figure(2)
plot(t,E,'k-');
xlabel('{\itTime} [s]','fontsize',12);
ylabel('{\itEnergy} [J]','fontsize',12);
title('{\itE} vs {\itt}','fontsize',14);
axis([0 max(t) 1.05*E0 0.95*E0]);

figure(3)
plot(t,Ax,'k-');
xlabel('{\itTime} [s]','fontsize',12);
ylabel('{\itAx}','fontsize',12);
title('{\itAx} vs {\itt}','fontsize',14);
axis([0 max(t) 0.5*Ax0 1.5*Ax0])

figure(4)
plot(t,Cx,'k-');
xlabel('{\itTime} [s]','fontsize',12);
```

```
ylabel('{\itCx}','fontsize',12);
title('{\itCx} vs {\itt}','fontsize',14);
axis([0 max(t) 0.749 0.751]);

figure(5)
plot(t,L,'k-');
xlabel('{\itTime} [s]','fontsize',12);
ylabel('{\itAngular momentum} [kgm^{2}s^{-1}]','fontsize',12);
title('{\itL} vs {\itt}','fontsize',14);
axis([0 max(t) -1.2*L0 1.2*L0]);
```

C.2 The 3D heavy Rydberg 'atom' simulation

```
clc; clear; clf;
Z=1;  k=8.99e9;  e=1.6e-19;          %Constants
mA=1.67e-27; mB=19*1.67e-27;         %ion masses

%A == H+, B == F-                    %Current masses entered

notimesteps = 100000;                %Number of timesteps
v = zeros(notimesteps,41);

Ex = 3e4; Ey = 0; Ez = 0;
Efield = sqrt(Ex^2 + Ey^2 + Ez^2);   %Electric field

%Initial conditions
t0  = 0;
h0  = 5e-14;       %Initial stepsize
xA0 = 28.5e-9;    %|
vxA0= 0;          %|
yA0 = 0;          %|
vyA0= 1900;       %|
zA0 = 0;          %|          Components of initial
vzA0= 0;          %|          positions and velocities
xB0 = -1.5e-9;    %|
vxB0= 0;          %|
yB0 = 0;          %|
vyB0= -100;       %|
zB0 = 0;          %|
vzB0= 0;          %|
rA0 = sqrt(xA0^2 + yA0^2 + zA0^2);      %Distance from origin
rB0 = sqrt(xB0^2 + yB0^2 + zB0^2);
Rx0 = (xA0 - xB0);                      %Separation of ions
Ry0 = (yA0 - yB0);
Rz0 = (zA0 - zB0);
R0  = sqrt(Rx0^2 + Ry0^2 + Rz0^2);
FxA0= -(k*Z*e^2)/R0^2*(Rx0/R0) - e*Ex;  %Force on A
FyA0= -(k*Z*e^2)/R0^2*(Ry0/R0) - e*Ey;
FzA0= -(k*Z*e^2)/R0^2*(Rz0/R0) - e*Ez;
FA0 = sqrt(FxA0^2 + FyA0^2 + FzA0^2);
FxB0= -FxA0;                            %Force on B
FyB0= -FyA0;
FzB0= -FzA0;
FB0 = sqrt(FxB0^2 + FyB0^2 + FzB0^2);
TA0 = mA/2*(vxA0^2 + vyA0^2 + vzA0^2);  %Kinetic energies
TB0 = mB/2*(vxB0^2 + vyB0^2 + vzB0^2);
U0  = -(k*Z*e^2)/R0 + e*(Ex*xA0 + Ey*yA0 + Ez*zA0) - e*(Ex*xB0 + Ey*yB0 + Ez*zB0);
E0  = TA0 + TB0 + U0;                   %Total energy
LxA0= mA*(yA0*vzA0 - zA0*vyA0);         %Angular momentum of A
LyA0= mA*(zA0*vxA0 - xA0*vzA0);
LzA0= mA*(xA0*vyA0 - yA0*vxA0);
LA0 = sqrt(LxA0^2 + LyA0^2 + LzA0^2);
LxB0= mB*(yB0*vzB0 - zB0*vyB0);         %Angular momentum of B
LyB0= mB*(zB0*vxB0 - xB0*vzB0);
```

```
LzB0= mB*(xB0*vyB0 - yB0*vxB0);
LB0 = sqrt(LxB0^2 + LyB0^2 + LzB0^2);
L0  = LA0 + LB0;                          %Total angular momentum

tmax = 5e-9;               %End simulation

v(1,1) = t0;       %1st row matrix entries
v(1,2) = h0;
v(1,3) = xA0;
v(1,4) = vxA0;
v(1,5) = yA0;
v(1,6) = vyA0;
v(1,7) = zA0;
v(1,8) = vzA0;
v(1,9) = xB0;
v(1,10)= vxB0;
v(1,11)= yB0;
v(1,12)= vyB0;
v(1,13)= zB0;
v(1,14)= vzB0;
v(1,15)= rA0;
v(1,16)= rB0;
v(1,17)= Rx0;
v(1,18)= Ry0;
v(1,19)= Rz0;
v(1,20)= R0;
v(1,21)= FxA0;
v(1,22)= FyA0;
v(1,23)= FzA0;
v(1,24)= FA0;
v(1,25)= FxB0;
v(1,26)= FyB0;
v(1,27)= FzB0;
v(1,28)= FB0;
v(1,29)= TA0;
v(1,30)= TB0;
v(1,31)= U0;
v(1,32)= E0;
v(1,33)= LxA0;
v(1,34)= LyA0;
v(1,35)= LzA0;
v(1,36)= LA0;
v(1,37)= LxB0;
v(1,38)= LyB0;
v(1,39)= LzB0;
v(1,40)= LB0;
v(1,41)= L0;

for n = (2:notimesteps)

    if   v(n-1,20) > 10*R0   %If R > 10*R0, end loop
       disp('R > 10R0'); break
    end
```

```
if   v(n-1,1) > tmax     %If t > tmax, end loop
   disp('t > tmax'); break
end

%Time (t)
v(n,1) = v(n-1,1) + (v(n-1,20)/R0)^2*h0;  %Adaptive stepsize

%Stepsize (h)
v(n,2)= v(n,1) - v(n-1,1);

%The Runge-Kutta algorithm

pA1 = v(n-1,4);          %dxA/dt = vxA
qA1 = -(k*Z*e^2)/v(n-1,20)^2/mA*v(n-1,17)/v(n-1,20) - e*Ex/mA;  %dvxA/dt = FxA/mA
rA1 = v(n-1,6);          %dyA/dt = vyA
sA1 = -(k*Z*e^2)/v(n-1,20)^2/mA*v(n-1,18)/v(n-1,20) - e*Ey/mA;  %dvyA/dt = FyA/mA
tA1 = v(n-1,8);          %dzA/dt = vzA
uA1 = -(k*Z*e^2)/v(n-1,20)^2/mA*v(n-1,19)/v(n-1,20) - e*Ez/mA;  %dvzA/dt = FzA/mA

pB1 = v(n-1,10);         %dxB/dt = vxB
qB1 = (k*Z*e^2)/v(n-1,20)^2/mB*v(n-1,17)/v(n-1,20) + e*Ex/mB;  %dvxB/dt = FxB/mB
rB1 = v(n-1,12);         %dyB/dt = vyB
sB1 = (k*Z*e^2)/v(n-1,20)^2/mB*v(n-1,18)/v(n-1,20) + e*Ey/mB;  %dvyB/dt = FyB/mB
tB1 = v(n-1,14);         %dzB/dt = vzB
uB1 = (k*Z*e^2)/v(n-1,20)^2/mB*v(n-1,19)/v(n-1,20) + e*Ez/mB;  %dvzB/dt = FzB/mB

pA2 = v(n-1,4) + v(n,2)/2*qA1;
qA2 = -(k*Z*e^2)/(((v(n-1,3) + v(n,2)/2*pA1) - (v(n-1,9) + v(n,2)/2*pB1))^2 + ...
                  ((v(n-1,5) + v(n,2)/2*rA1) - (v(n-1,11) + v(n,2)/2*rB1))^2 + ...
                  ((v(n-1,7) + v(n,2)/2*tA1) - (v(n-1,13) + v(n,2)/2*tB1))^2)/mA*...
                  ((v(n-1,3) + v(n,2)/2*pA1) - (v(n-1,9) + v(n,2)/2*pB1))/...
                  (((v(n-1,3) + v(n,2)/2*pA1) - (v(n-1,9) + v(n,2)/2*pB1))^2 + ...
                  ((v(n-1,5) + v(n,2)/2*rA1) - (v(n-1,11) + v(n,2)/2*rB1))^2 + ...
      ((v(n-1,7) + v(n,2)/2*tA1) - (v(n-1,13) + v(n,2)/2*tB1))^2)^(1/2) - e*Ex/mA;
rA2 = v(n-1,6) + v(n,2)/2*sA1;
sA2 = -(k*Z*e^2)/(((v(n-1,3) + v(n,2)/2*pA1) - (v(n-1,9) + v(n,2)/2*pB1))^2 + ...
                  ((v(n-1,5) + v(n,2)/2*rA1) - (v(n-1,11) + v(n,2)/2*rB1))^2 + ...
                  ((v(n-1,7) + v(n,2)/2*tA1) - (v(n-1,13) + v(n,2)/2*tB1))^2)/mA*...
                  ((v(n-1,5) + v(n,2)/2*rA1) - (v(n-1,11) + v(n,2)/2*rB1))/...
                  (((v(n-1,3) + v(n,2)/2*pA1) - (v(n-1,9) + v(n,2)/2*pB1))^2 + ...
                  ((v(n-1,5) + v(n,2)/2*rA1) - (v(n-1,11) + v(n,2)/2*rB1))^2 + ...
      ((v(n-1,7) + v(n,2)/2*tA1) - (v(n-1,13) + v(n,2)/2*tB1))^2)^(1/2) - e*Ey/mA;
tA2 = v(n-1,8) + v(n,2)/2*uA1;
uA2 = -(k*Z*e^2)/(((v(n-1,3) + v(n,2)/2*pA1) - (v(n-1,9) + v(n,2)/2*pB1))^2 + ...
                  ((v(n-1,5) + v(n,2)/2*rA1) - (v(n-1,11) + v(n,2)/2*rB1))^2 + ...
                  ((v(n-1,7) + v(n,2)/2*tA1) - (v(n-1,13) + v(n,2)/2*tB1))^2)/mA*...
                  ((v(n-1,7) + v(n,2)/2*tA1) - (v(n-1,13) + v(n,2)/2*tB1))/...
                  (((v(n-1,3) + v(n,2)/2*pA1) - (v(n-1,9) + v(n,2)/2*pB1))^2 + ...
                  ((v(n-1,5) + v(n,2)/2*rA1) - (v(n-1,11) + v(n,2)/2*rB1))^2 + ...
      ((v(n-1,7) + v(n,2)/2*tA1) - (v(n-1,13) + v(n,2)/2*tB1))^2)^(1/2) - e*Ez/mA;

pB2 = v(n-1,10) + v(n,2)/2*qB1;
qB2 = (k*Z*e^2)/(((v(n-1,3) + v(n,2)/2*pA1) - (v(n-1,9) + v(n,2)/2*pB1))^2 + ...
                  ((v(n-1,5) + v(n,2)/2*rA1) - (v(n-1,11) + v(n,2)/2*rB1))^2 + ...
```

```
                ((v(n-1,7) + v(n,2)/2*tA1) - (v(n-1,13) + v(n,2)/2*tB1))^2)/mB*...
                ((v(n-1,3) + v(n,2)/2*pA1) - (v(n-1,9) + v(n,2)/2*pB1))/...
                (((v(n-1,3) + v(n,2)/2*pA1) - (v(n-1,9) + v(n,2)/2*pB1))^2 + ...
                ((v(n-1,5) + v(n,2)/2*rA1) - (v(n-1,11) + v(n,2)/2*rB1))^2 + ...
      ((v(n-1,7) + v(n,2)/2*tA1) - (v(n-1,13) + v(n,2)/2*tB1))^2)^(1/2) + e*Ex/mB;
rB2 = v(n-1,12) + v(n,2)/2*sB1;
sB2 = (k*Z*e^2)/(((v(n-1,3) + v(n,2)/2*pA1) - (v(n-1,9) + v(n,2)/2*pB1))^2 + ...
                ((v(n-1,5) + v(n,2)/2*rA1) - (v(n-1,11) + v(n,2)/2*rB1))^2 + ...
                ((v(n-1,7) + v(n,2)/2*tA1) - (v(n-1,13) + v(n,2)/2*tB1))^2)/mB*...
                ((v(n-1,5) + v(n,2)/2*rA1) - (v(n-1,11) + v(n,2)/2*rB1))/...
                (((v(n-1,3) + v(n,2)/2*pA1) - (v(n-1,9) + v(n,2)/2*pB1))^2 + ...
                ((v(n-1,5) + v(n,2)/2*rA1) - (v(n-1,11) + v(n,2)/2*rB1))^2 + ...
      ((v(n-1,7) + v(n,2)/2*tA1) - (v(n-1,13) + v(n,2)/2*tB1))^2)^(1/2) + e*Ey/mB;
tB2 = v(n-1,14) + v(n,2)/2*uB1;
uB2 = (k*Z*e^2)/(((v(n-1,3) + v(n,2)/2*pA1) - (v(n-1,9) + v(n,2)/2*pB1))^2 + ...
                ((v(n-1,5) + v(n,2)/2*rA1) - (v(n-1,11) + v(n,2)/2*rB1))^2 + ...
                ((v(n-1,7) + v(n,2)/2*tA1) - (v(n-1,13) + v(n,2)/2*tB1))^2)/mB*...
                ((v(n-1,7) + v(n,2)/2*rA1) - (v(n-1,13) + v(n,2)/2*rB1))/...
                (((v(n-1,3) + v(n,2)/2*pA1) - (v(n-1,9) + v(n,2)/2*pB1))^2 + ...
                ((v(n-1,5) + v(n,2)/2*rA1) - (v(n-1,11) + v(n,2)/2*rB1))^2 + ...
      ((v(n-1,7) + v(n,2)/2*tA1) - (v(n-1,13) + v(n,2)/2*tB1))^2)^(1/2) + e*Ez/mB;

pA3 = v(n-1,4) + v(n,2)/2*qA2;
qA3 = -(k*Z*e^2)/(((v(n-1,3) + v(n,2)/2*pA2) - (v(n-1,9) + v(n,2)/2*pB2))^2 + ...
                ((v(n-1,5) + v(n,2)/2*rA2) - (v(n-1,11) + v(n,2)/2*rB2))^2 + ...
                ((v(n-1,7) + v(n,2)/2*tA2) - (v(n-1,13) + v(n,2)/2*tB2))^2)/mA*...
                ((v(n-1,3) + v(n,2)/2*pA2) - (v(n-1,9) + v(n,2)/2*pB2))/...
                (((v(n-1,3) + v(n,2)/2*pA2) - (v(n-1,9) + v(n,2)/2*pB2))^2 + ...
                ((v(n-1,5) + v(n,2)/2*rA2) - (v(n-1,11) + v(n,2)/2*rB2))^2 + ...
      ((v(n-1,7) + v(n,2)/2*tA2) - (v(n-1,13) + v(n,2)/2*tB2))^2)^(1/2) - e*Ex/mA;
rA3 = v(n-1,6) + v(n,2)/2*sA2;
sA3 = -(k*Z*e^2)/(((v(n-1,3) + v(n,2)/2*pA2) - (v(n-1,9) + v(n,2)/2*pB2))^2 + ...
                ((v(n-1,5) + v(n,2)/2*rA2) - (v(n-1,11) + v(n,2)/2*rB2))^2 + ...
                ((v(n-1,7) + v(n,2)/2*tA2) - (v(n-1,13) + v(n,2)/2*tB2))^2)/mA*...
                ((v(n-1,5) + v(n,2)/2*rA2) - (v(n-1,11) + v(n,2)/2*rB2))/...
                (((v(n-1,3) + v(n,2)/2*pA2) - (v(n-1,9) + v(n,2)/2*pB2))^2 + ...
                ((v(n-1,5) + v(n,2)/2*rA2) - (v(n-1,11) + v(n,2)/2*rB2))^2 + ...
      ((v(n-1,7) + v(n,2)/2*tA2) - (v(n-1,13) + v(n,2)/2*tB2))^2)^(1/2) - e*Ey/mA;
tA3 = v(n-1,8) + v(n,2)/2*uA2;
uA3 = -(k*Z*e^2)/(((v(n-1,3) + v(n,2)/2*pA2) - (v(n-1,9) + v(n,2)/2*pB2))^2 + ...
                ((v(n-1,5) + v(n,2)/2*rA2) - (v(n-1,11) + v(n,2)/2*rB2))^2 + ...
                ((v(n-1,7) + v(n,2)/2*tA2) - (v(n-1,13) + v(n,2)/2*tB2))^2)/mA*...
                ((v(n-1,7) + v(n,2)/2*tA2) - (v(n-1,13) + v(n,2)/2*tB2))/...
                (((v(n-1,3) + v(n,2)/2*pA2) - (v(n-1,9) + v(n,2)/2*pB2))^2 + ...
                ((v(n-1,5) + v(n,2)/2*rA2) - (v(n-1,11) + v(n,2)/2*rB2))^2 + ...
      ((v(n-1,7) + v(n,2)/2*tA2) - (v(n-1,13) + v(n,2)/2*tB2))^2)^(1/2) - e*Ez/mA;

pB3 = v(n-1,10) + v(n,2)/2*qB2;
qB3 = (k*Z*e^2)/(((v(n-1,3) + v(n,2)/2*pA2) - (v(n-1,9) + v(n,2)/2*pB2))^2 + ...
                ((v(n-1,5) + v(n,2)/2*rA2) - (v(n-1,11) + v(n,2)/2*rB2))^2 + ...
                ((v(n-1,7) + v(n,2)/2*tA2) - (v(n-1,13) + v(n,2)/2*tB2))^2)/mB*...
                ((v(n-1,3) + v(n,2)/2*pA2) - (v(n-1,9) + v(n,2)/2*pB2))/...
                (((v(n-1,3) + v(n,2)/2*pA2) - (v(n-1,9) + v(n,2)/2*pB2))^2 + ...
                ((v(n-1,5) + v(n,2)/2*rA2) - (v(n-1,11) + v(n,2)/2*rB2))^2 + ...
```

```
      ((v(n-1,7) + v(n,2)/2*tA2) - (v(n-1,13) + v(n,2)/2*tB2))^2)^(1/2) + e*Ex/mB;
rB3 = v(n-1,12) + v(n,2)/2*sB2;
sB3 = (k*Z*e^2)/(((v(n-1,3) + v(n,2)/2*pA2) - (v(n-1,9) + v(n,2)/2*pB2))^2 + ...
                 ((v(n-1,5) + v(n,2)/2*rA2) - (v(n-1,11) + v(n,2)/2*rB2))^2 + ...
                 ((v(n-1,7) + v(n,2)/2*tA2) - (v(n-1,13) + v(n,2)/2*tB2))^2)/mB*...
                 ((v(n-1,5) + v(n,2)/2*rA2) - (v(n-1,11) + v(n,2)/2*rB2))/...
                 (((v(n-1,3) + v(n,2)/2*pA2) - (v(n-1,9) + v(n,2)/2*pB2))^2 + ...
                 ((v(n-1,5) + v(n,2)/2*rA2) - (v(n-1,11) + v(n,2)/2*rB2))^2 + ...
      ((v(n-1,7) + v(n,2)/2*tA2) - (v(n-1,13) + v(n,2)/2*tB2))^2)^(1/2) + e*Ey/mB;
tB3 = v(n-1,14) + v(n,2)/2*uB2;
uB3 = (k*Z*e^2)/(((v(n-1,3) + v(n,2)/2*pA2) - (v(n-1,9) + v(n,2)/2*pB2))^2 + ...
                 ((v(n-1,5) + v(n,2)/2*rA2) - (v(n-1,11) + v(n,2)/2*rB2))^2 + ...
                 ((v(n-1,7) + v(n,2)/2*tA2) - (v(n-1,13) + v(n,2)/2*tB2))^2)/mB*...
                 ((v(n-1,7) + v(n,2)/2*rA2) - (v(n-1,13) + v(n,2)/2*rB2))/...
                 (((v(n-1,3) + v(n,2)/2*pA2) - (v(n-1,9) + v(n,2)/2*pB2))^2 + ...
                 ((v(n-1,5) + v(n,2)/2*rA2) - (v(n-1,11) + v(n,2)/2*rB2))^2 + ...
      ((v(n-1,7) + v(n,2)/2*tA2) - (v(n-1,13) + v(n,2)/2*tB2))^2)^(1/2) + e*Ez/mB;

pA4 = v(n-1,4) + v(n,2)*qA3;
qA4 = -(k*Z*e^2)/(((v(n-1,3) + v(n,2)*pA3) - (v(n-1,9) + v(n,2)*pB3))^2 + ...
                 ((v(n-1,5) + v(n,2)*rA3) - (v(n-1,11) + v(n,2)*rB3))^2 + ...
                 ((v(n-1,7) + v(n,2)*tA3) - (v(n-1,13) + v(n,2)*tB3))^2)/mA*...
                 ((v(n-1,3) + v(n,2)*pA3) - (v(n-1,9) + v(n,2)*pB3))/...
                 (((v(n-1,3) + v(n,2)*pA3) - (v(n-1,9) + v(n,2)*pB3))^2 + ...
                 ((v(n-1,5) + v(n,2)*rA3) - (v(n-1,11) + v(n,2)*rB3))^2 + ...
      ((v(n-1,7) + v(n,2)*tA3) - (v(n-1,13) + v(n,2)*tB3))^2)^(1/2) - e*Ex/mA;
rA4 = v(n-1,6) + v(n,2)*sA3;
sA4 = -(k*Z*e^2)/(((v(n-1,3) + v(n,2)*pA3) - (v(n-1,9) + v(n,2)*pB3))^2 + ...
                 ((v(n-1,5) + v(n,2)*rA3) - (v(n-1,11) + v(n,2)*rB3))^2 + ...
                 ((v(n-1,7) + v(n,2)*tA3) - (v(n-1,13) + v(n,2)*tB3))^2)/mA*...
                 ((v(n-1,5) + v(n,2)*rA3) - (v(n-1,11) + v(n,2)*rB3))/...
                 (((v(n-1,3) + v(n,2)*pA3) - (v(n-1,9) + v(n,2)*pB3))^2 + ...
                 ((v(n-1,5) + v(n,2)*rA3) - (v(n-1,11) + v(n,2)*rB3))^2 + ...
      ((v(n-1,7) + v(n,2)*tA3) - (v(n-1,13) + v(n,2)*tB3))^2)^(1/2) - e*Ey/mA;
tA4 = v(n-1,8) + v(n,2)*uA3;
uA4 = -(k*Z*e^2)/(((v(n-1,3) + v(n,2)*pA3) - (v(n-1,9) + v(n,2)*pB3))^2 + ...
                 ((v(n-1,5) + v(n,2)*rA3) - (v(n-1,11) + v(n,2)*rB3))^2 + ...
                 ((v(n-1,7) + v(n,2)*tA3) - (v(n-1,13) + v(n,2)*tB3))^2)/mA*...
                 ((v(n-1,7) + v(n,2)*tA3) - (v(n-1,13) + v(n,2)*tB3))/...
                 (((v(n-1,3) + v(n,2)*pA3) - (v(n-1,9) + v(n,2)*pB3))^2 + ...
                 ((v(n-1,5) + v(n,2)*rA3) - (v(n-1,11) + v(n,2)*rB3))^2 + ...
      ((v(n-1,7) + v(n,2)*tA3) - (v(n-1,13) + v(n,2)*tB3))^2)^(1/2) - e*Ez/mA;

pB4 = v(n-1,10) + v(n,2)*qB3;
qB4 = (k*Z*e^2)/(((v(n-1,3) + v(n,2)*pA3) - (v(n-1,9) + v(n,2)*pB3))^2 + ...
                 ((v(n-1,5) + v(n,2)*rA3) - (v(n-1,11) + v(n,2)*rB3))^2 + ...
                 ((v(n-1,7) + v(n,2)*tA3) - (v(n-1,13) + v(n,2)*tB3))^2)/mB*...
                 ((v(n-1,3) + v(n,2)*pA3) - (v(n-1,9) + v(n,2)*pB3))/...
                 (((v(n-1,3) + v(n,2)*pA3) - (v(n-1,9) + v(n,2)*pB3))^2 + ...
                 ((v(n-1,5) + v(n,2)*rA3) - (v(n-1,11) + v(n,2)*rB3))^2 + ...
      ((v(n-1,7) + v(n,2)*tA3) - (v(n-1,13) + v(n,2)*tB3))^2)^(1/2) + e*Ex/mB;
rB4 = v(n-1,12) + v(n,2)*sB3;
sB4 = (k*Z*e^2)/(((v(n-1,3) + v(n,2)*pA3) - (v(n-1,9) + v(n,2)*pB3))^2 + ...
                 ((v(n-1,5) + v(n,2)*rA3) - (v(n-1,11) + v(n,2)*rB3))^2 + ...
```

```
                ((v(n-1,7) + v(n,2)*tA3) - (v(n-1,13) + v(n,2)*tB3))^2)/mB*...
                ((v(n-1,5) + v(n,2)*rA3) - (v(n-1,11) + v(n,2)*rB3))/...
                (((v(n-1,3) + v(n,2)*pA3) - (v(n-1,9) + v(n,2)*pB3))^2 + ...
                ((v(n-1,5) + v(n,2)*rA3) - (v(n-1,11) + v(n,2)*rB3))^2 + ...
      ((v(n-1,7) + v(n,2)*tA3) - (v(n-1,13) + v(n,2)*tB3))^2)^(1/2) + e*Ey/mB;
tB4 = v(n-1,14) + v(n,2)*uB3;
uB4 = (k*Z*e^2)/(((v(n-1,3) + v(n,2)*pA3) - (v(n-1,9) + v(n,2)*pB3))^2 + ...
                ((v(n-1,5) + v(n,2)*rA3) - (v(n-1,11) + v(n,2)*rB3))^2 + ...
                ((v(n-1,7) + v(n,2)*tA3) - (v(n-1,13) + v(n,2)*tB3))^2)/mB*...
                ((v(n-1,7) + v(n,2)*rA3) - (v(n-1,13) + v(n,2)*rB3))/...
                (((v(n-1,3) + v(n,2)*pA3) - (v(n-1,9) + v(n,2)*pB3))^2 + ...
                ((v(n-1,5) + v(n,2)*rA3) - (v(n-1,11) + v(n,2)*rB3))^2 + ...
      ((v(n-1,7) + v(n,2)*tA3) - (v(n-1,13) + v(n,2)*tB3))^2)^(1/2) + e*Ez/mB;

%xA
v(n,3) = v(n-1,3) + (v(n,2)/6)*(pA1 + 2*pA2 + 2*pA3 + pA4);

%vxA
v(n,4) = v(n-1,4) + (v(n,2)/6)*(qA1 + 2*qA2 + 2*qA3 + qA4);

%yA
v(n,5) = v(n-1,5) + (v(n,2)/6)*(rA1 + 2*rA2 + 2*rA3 + rA4);

%vyA
v(n,6) = v(n-1,6) + (v(n,2)/6)*(sA1 + 2*sA2 + 2*sA3 + sA4);

%zA
v(n,7) = v(n-1,7) + (v(n,2)/6)*(tA1 + 2*tA2 + 2*tA3 + tA4);

%vzA
v(n,8) = v(n-1,8) + (v(n,2)/6)*(uA1 + 2*uA2 + 2*uA3 + uA4);

%xB
v(n,9) = v(n-1,9) + (v(n,2)/6)*(pB1 + 2*pB2 + 2*pB3 + pB4);

%vxB
v(n,10)= v(n-1,10) + (v(n,2)/6)*(qB1 + 2*qB2 + 2*qB3 + qB4);

%yB
v(n,11)= v(n-1,11) + (v(n,2)/6)*(rB1 + 2*rB2 + 2*rB3 + rB4);

%vyB
v(n,12)= v(n-1,12) + (v(n,2)/6)*(sB1 + 2*sB2 + 2*sB3 + sB4);

%zB
v(n,13)= v(n-1,13) + (v(n,2)/6)*(tB1 + 2*tB2 + 2*tB3 + tB4);

%vzB
v(n,14)= v(n-1,14) + (v(n,2)/6)*(uB1 + 2*uB2 + 2*uB3 + uB4);

%rA    % from origin
v(n,15)= sqrt(v(n,3)^2 + v(n,5)^2 + v(n,7)^2);

%rB    % from origin
```

```
v(n,16)= sqrt(v(n,9)^2 + v(n,11)^2 + v(n,13)^2);

%Rx    % from other ion
v(n,17)= v(n,3) - v(n,9);

%Ry    % from other ion
v(n,18)= v(n,5) - v(n,11);

%Rz    % from other ion
v(n,19)= v(n,7) - v(n,13);

%R     % from other ion
v(n,20)= sqrt(v(n,17)^2 + v(n,18)^2 + v(n,19)^2);

%FxA
v(n,21)= -k*Z*e^2/v(n,20)^2*(v(n,17)/v(n,20)) - e*Ex;

%FyA
v(n,22)= -k*Z*e^2/v(n,20)^2*(v(n,18)/v(n,20)) - e*Ey;

%FzA
v(n,23)= -k*Z*e^2/v(n,20)^2*(v(n,19)/v(n,20)) - e*Ez;

%FA
v(n,24)= sqrt(v(n,21)^2 + v(n,22)^2 + v(n,23)^2);

%FxB
v(n,25)= k*Z*e^2/v(n,20)^2*(v(n,17)/v(n,20)) + e*Ex;

%FyB
v(n,26)= k*Z*e^2/v(n,20)^2*(v(n,18)/v(n,20)) + e*Ey;

%FyB
v(n,27)= k*Z*e^2/v(n,20)^2*(v(n,19)/v(n,20)) + e*Ez;

%FB
v(n,28)= sqrt(v(n,25)^2 + v(n,26)^2 + v(n,27)^2);

%TA (KE)
v(n,29)= (mA/2)*(v(n,4)^2 + v(n,6)^2 + v(n,8)^2);

%TB (KE)
v(n,30)= (mB/2)*(v(n,10)^2 + v(n,12)^2 + v(n,14)^2);

%U (PE)
v(n,31)= -(k*Z*e^2)/v(n,20) + e*(Ex*v(n,3) + Ey*v(n,5) + Ez*v(n,7)) - ...
                              e*(Ex*v(n,9) + Ey*v(n,11) + Ez*v(n,13));

%E
v(n,32)= v(n,29) + v(n,30) + v(n,31);

%LxA
v(n,33)= mA*(v(n,5)*v(n,8) - v(n,7)*v(n,6));
```

```
    %LyA
    v(n,34)= mA*(v(n,7)*v(n,4) - v(n,3)*v(n,8));

    %LzA
    v(n,35)= mA*(v(n,3)*v(n,6) - v(n,5)*v(n,4));

    %LA
    v(n,36)= sqrt(v(n,33)^2 + v(n,34)^2 + v(n,35)^2);

    %LxB
    v(n,37)= mB*(v(n,11)*v(n,14) - v(n,13)*v(n,12));

    %LyB
    v(n,38)= mB*(v(n,13)*v(n,10) - v(n,9)*v(n,14));

    %LzB
    v(n,39)= mB*(v(n,9)*v(n,12) - v(n,11)*v(n,10));

    %LB
    v(n,40)= sqrt(v(n,37)^2 + v(n,38)^2 + v(n,39)^2);

    %L
    v(n,41)= v(n,36) + v(n,40);

end

format short g;

w = v(1:n-1,:);

%disp('       t        h        x        y        E');       %Display output
%W = [w(:,1),w(:,2),w(:,3),w(:,5),w(:,32)];
%disp(W);

t  = w(:,1);
h  = w(:,2);
xA = w(:,3);
vxA= w(:,4);
yA = w(:,5);
vyA= w(:,6);
zA = w(:,7);
vzA= w(:,8);
xB = w(:,9);
vxB= w(:,10);
yB = w(:,11);
vyB= w(:,12);
zB = w(:,13);
vzB= w(:,14);
rA = w(:,15);
rB = w(:,16);
Rx = w(:,17);
Ry = w(:,18);
Rz = w(:,19);
R  = w(:,20);
```

```
FxA= w(:,21);
FyA= w(:,22);
FzA= w(:,23);
FA = w(:,24);
FxB= w(:,25);
FyB= w(:,26);
FzB= w(:,27);
FB = w(:,28);
TA = w(:,29);
TB = w(:,30);
U  = w(:,31);
E  = w(:,32);
LxA= w(:,33);
LyA= w(:,34);
LzA= w(:,35);
LA = w(:,36);
LxB= w(:,37);
LyB= w(:,38);
LzB= w(:,39);
LB = w(:,40);
L  = w(:,41);


disp(n)        %Display no. of final timestep reached
disp(w(n-1,1)) %Display final time


apo = max(r);            %Apogee      Envelope calculations
peri= min(r);            %Perigee
majoraxis = apo + peri;  %Majoraxis

disp('    Apogee       Perigee       major-axis')
P = [apo,peri,majoraxis];
disp(P);


%Plotting figures

figure(1)
subplot(1,3,1); plot(xA,yA,'r-',xB,yB,'b-'); axis equal;
xlabel('{\itx} position [m]','fontsize',12);
ylabel('{\ity} position [m]','fontsize',12);
title('{\ity} vs {\itx}','fontsize',14);
legend('H^+','F^-');
subplot(1,3,2); plot(xA,zA,'r-',xB,zB,'b-'); axis equal;
xlabel('{\itx} position [m]','fontsize',10);
ylabel('{\itz} position [m]','fontsize',10);
title('{\itz} vs {\itx}','fontsize',12);
subplot(1,3,3); plot(yA,zA,'r-',yB,zB,'b-'); axis equal;
xlabel('{\ity} position [m]','fontsize',10);
ylabel('{\itz} position [m]','fontsize',10);
title('{\itz} vs {\ity}','fontsize',12);

figure(2)
```

```
subplot(3,2,1); plot(xA,yA,'k-'); axis equal;
xlabel('{\itx_A} [m]','fontsize',10);
ylabel('{\ity_A} [m]','fontsize',10);
title('{\ity_A} vs {\itx_A}','fontsize',12);
subplot(3,2,2); plot(xA,zA,'k-'); axis equal;
xlabel('{\itx_A} [m]','fontsize',10);
ylabel('{\itz_A} [m]','fontsize',10);
title('{\itz_A} vs {\itx_A}','fontsize',12);
subplot(3,2,3); plot(yA,zA,'k-'); axis equal;
xlabel('{\ity_A} [m]','fontsize',10);
ylabel('{\itz_A} [m]','fontsize',10);
title('{\itz_A} vs {\ity_A}','fontsize',12);
subplot(3,2,4); plot(xB,yB,'k-'); axis equal;
xlabel('{\itx_B} [m]','fontsize',10);
ylabel('{\ity_B} [m]','fontsize',10);
title('{\ity_B} vs {\itx_B}','fontsize',12);
subplot(3,2,5); plot(xB,zB,'k-'); axis equal;
xlabel('{\itx_B} [m]','fontsize',10);
ylabel('{\itz_B} [m]','fontsize',10);
title('{\itz_B} vs {\itx_B}','fontsize',12);
subplot(3,2,6); plot(yB,zB,'k-'); axis equal;
xlabel('{\ity_B} [m]','fontsize',10);
ylabel('{\itz_B} [m]','fontsize',10);
title('{\itz_B} vs {\ity_B}','fontsize',12);

figure(3)
subplot(1,3,1); plot(Rx,Ry,'k-'); axis equal;
xlabel('{\itR_x} [m]','fontsize',10);
ylabel('{\itR_y} [m]','fontsize',10);
title('{\itR_y} vs {\itR_x}','fontsize',12);
subplot(1,3,2); plot(Rx,Rz,'k-'); axis equal;
xlabel('{\itR_x} [m]','fontsize',10);
ylabel('{\itR_z} [m]','fontsize',10);
title('{\itR_z} vs {\itR_x}','fontsize',12);
subplot(1,3,3); plot(Ry,Rz,'k-'); axis equal;
xlabel('{\itR_y} [m]','fontsize',10);
ylabel('{\itR_z} [m]','fontsize',12);
title('{\itR_z} vs {\itR_y}','fontsize',12);

figure(4)
subplot(1,3,1); plot(t,LA);
xlabel('{\itTime} [s]','fontsize',12);
ylabel('{\itL_A} [Js]','fontsize',12);
title('{\itL_A} vs {\itt}','fontsize',14);
axis([0 w(n-1,1) min(LA) max(LA)]);
subplot(1,3,2); plot(t,LB);
xlabel('{\itTime} [s]','fontsize',12);
ylabel('{\itL_B} [Js]','fontsize',12);
title('{\itL_B} vs {\itt}','fontsize',14);
axis([0 w(n-1,1) min(LB) max(LB)]);
subplot(1,3,3); plot(t,L);
xlabel('{\itTime} [s]','fontsize',12);
ylabel('{\Sigma\itL} [Js]','fontsize',12);
title('{\Sigma\itL} vs {\itt}','fontsize',14);
```

```
axis([0 w(n-1,1) min(L) max(L)]);

figure(5)
plot(t,R,'k-');
xlabel('{\itt} [s]','fontsize',12);
ylabel('{\itRadial separation} [m]','fontsize',12);
title('{\itR} vs {\itt}','fontsize',14);
axis([0 max(t) 0 max(R)]);

figure(6)
plot(t,E,'k-');
xlabel('{\itTime} [s]','fontsize',12);
ylabel('{\itE} [J]','fontsize',12);
title('{\itE} vs {\itt}','fontsize',14);
axis([0 max(t) min(E) max(E)])
```

Bibliography

[1] T. F. Gallagher, *Rydberg Atoms*
(Cambridge University Press, Cambridge, 1999).

[2] L. Holmlid, *A novel model for the interpretation of the unidentified infrared (UIR) bands from interstellar space: deexcitation of Rydberg Matter*
Astron. Astrophys. **358**, pp.276-286 (2000).

[3] R. C. Shiell, X. K. Hu, Q. J. Hu & J. W. Hepburn *Threshold Ion-Pair Production Spectroscopy*
http://www.chem.ubc.ca/faculty/hepburn/tipps.htm.

[4] J. B. Marion & S. T. Thornton, *Classical Dynamics of Particles and Systems*
(Cambridge University Press, Cambridge, 1999).

[5] H. A. Bethe & E. E. Salpeter, *Quantum Mechanics of One and Two Electron Systems*
(Springer, Berlin, 1957).

[6] L.Holmlid & Shahriar Badiei, *Rydberg matter in space: low-density condensed dark matter*
Monthly Notices R.A.S. **333**, vol.2 p.360 (2002).

[7] L. D. Landau & E. M. Lifshitz, *Mechanics (3rd edition)*
(Pergamon Press Ltd, Oxford, 1976).

[8] W. Lenz, *The evolution of the motions and quantum conditions of disturbed Keplerian motion*
Z. Physik **24** p.197 (1924).

[9] P. J. Redmond, *Generalization of the Runge-Lenz Vector in the Presence of an Electric Field*
Physical Review **133** No.5B, pp.B1352-B1353 (1964).

[10] H. Kopka & P. W. Daly, *A Guide to LaTeX*
(Addison-Wesley, Reading, 1994).

[11] T. P. Hezel, C. E. Burkhardt, M. Ciocca & J. J. Leventhal, *Classical View of the Stark Effect in Hydrogen Atoms*
Am. J. Phys. **60** No.4, pp.324-328 (1992).

[12] E. Neumann, *My Physics Lab - Graphical Simulations*
http://www.myphysicslab.com/.

[13] E. Reinhold, W. Ubachs, *Observation of coherent wave packets in a heavy Rydberg system*
Phys. Rev. Lett. **88** No.4, 013001 (2002).

[14] *The Runge-Kutta Algorithm*
http://www.krellinst.org/UCES/archive/modules/diffeq/node10.html.

[15] http://www.site.uottawa.ca:4321/astronomy/index.html#autoionization.

[16] *The Quantum Mechanical Hydrogen Atom in Parabolic Coordinates*
http://www.umsl.edu/ jjl/P471/4aseparation.pdf.